Interaction des radionucléides (actinides) dans l'environnement

C. Den Auwer

Université Côte d'Azur, Institut de Chimie de Nice

1. Natural / anthropogenic radionuclides

- 1.1 Definitions
- 1.2 Natural uranium
- 1.3 Anthropogenic radioactivity in the atmosphere
- 1.4 Oceans and seas

2. Uranium, Neptunium and plutonium chemistry in the environment

- 2.1 General trends
- 2.2 Hydrolysis
- 2.3 Actinide minerals in NORM

3. Speciation and speciation tools in natural environment

- 3.1 X-ray Asorption Spectroscopy
- 3.2 Accelerated Mass Spectroscopy
- 3.3 The specific case of seawater

1. Natural / anthropogenic radionuclides

1.1 Definitions

✔ **Cosmogenic radionuclides** : radionuclides produced by the intercation of cosmic radiations with the gaseous and particulate constituents of earth atmosphere.

- produced by spallation, neutron capture, muon capture.

✔ **Primordial radionuclides** : radioisotopes which half-lives comparable or larger than the age of Earth (4.5 10^9 years).

✔ **Radionuclides from natural decay series**

3 series (+ 1 already gone, 237Np) : 232Th, 238U, 235U

- they originate from primordial radionuclides with half-life > 5 10^8 years
- they possess a gaseous radioisotope of Rn
- They end with stable Pb
- They decay via a series of α and β transformations

NORM : Naturally Occuring Radioactive Materials

✔ **Technically enhances naturally occuring radioactive materials** (TENORM) : concentration of NORM modified to be used in cusmer products and other human adapations : Mining, fertilizer, fossil fuel ....

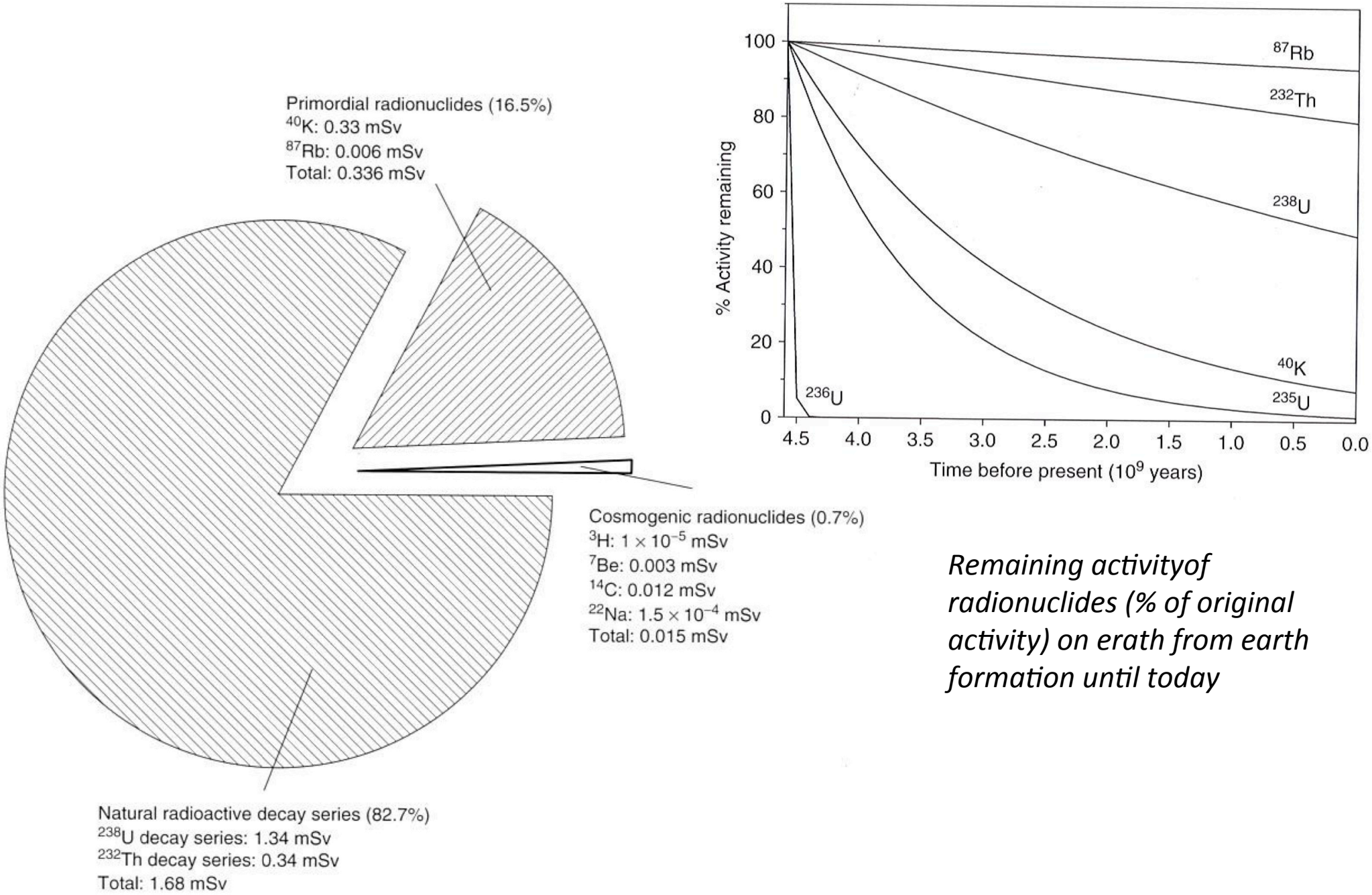

Remaining activityof radionuclides (% of original activity) on erath from earth formation until today

World average annual dose and percentage contribution to the dose from natural radionuclides

Radionuclides in the Environment, D.A. Atwood, Wiley 2010

1.2 Natural uranium

✔ Natural Uranium

238-U = 99.275 %
235-U = 0.711 %
234-U = 0.0056 %

Half life of uranium-234 : 2.46 x 10^5 years
Half life of uranium-235 : 7.04 x 10^8 years
Half life of uranium-238 : 4.47 x 10^9 years

Secular equilibrium obtained at about 10 times the half life (T) of the son of the largest T
For 238-U : 234-U (T=2.46 10^5 years)
=> 2 10^6 years

Very high-grade ore (Canada) – 20% U	200,000 ppm U
High-grade ore – 2% U,	20,000 ppm U
Low-grade ore – 0.1% U,	1,000 ppm U
Very low-grade ore* (Namibia)	0.01% U 100 ppm U
Granite	3-5 ppm U
Sedimentary rock	2-3 ppm U
Earth's continental crust (av)	2.8 ppm U
Seawater	0.003 ppm U

✔ Natural uranium is abundant in seawater

Uranium concentration may be calculated (empirically) from salinity

$$^{238}U\ (Bq.l^{-1}) = (\ 0{,}0713\ \pm 0{,}0012\ ) \times \frac{salinité}{60}$$

Marine Chem. (2007), 106, 530.

238-uranium decay chain

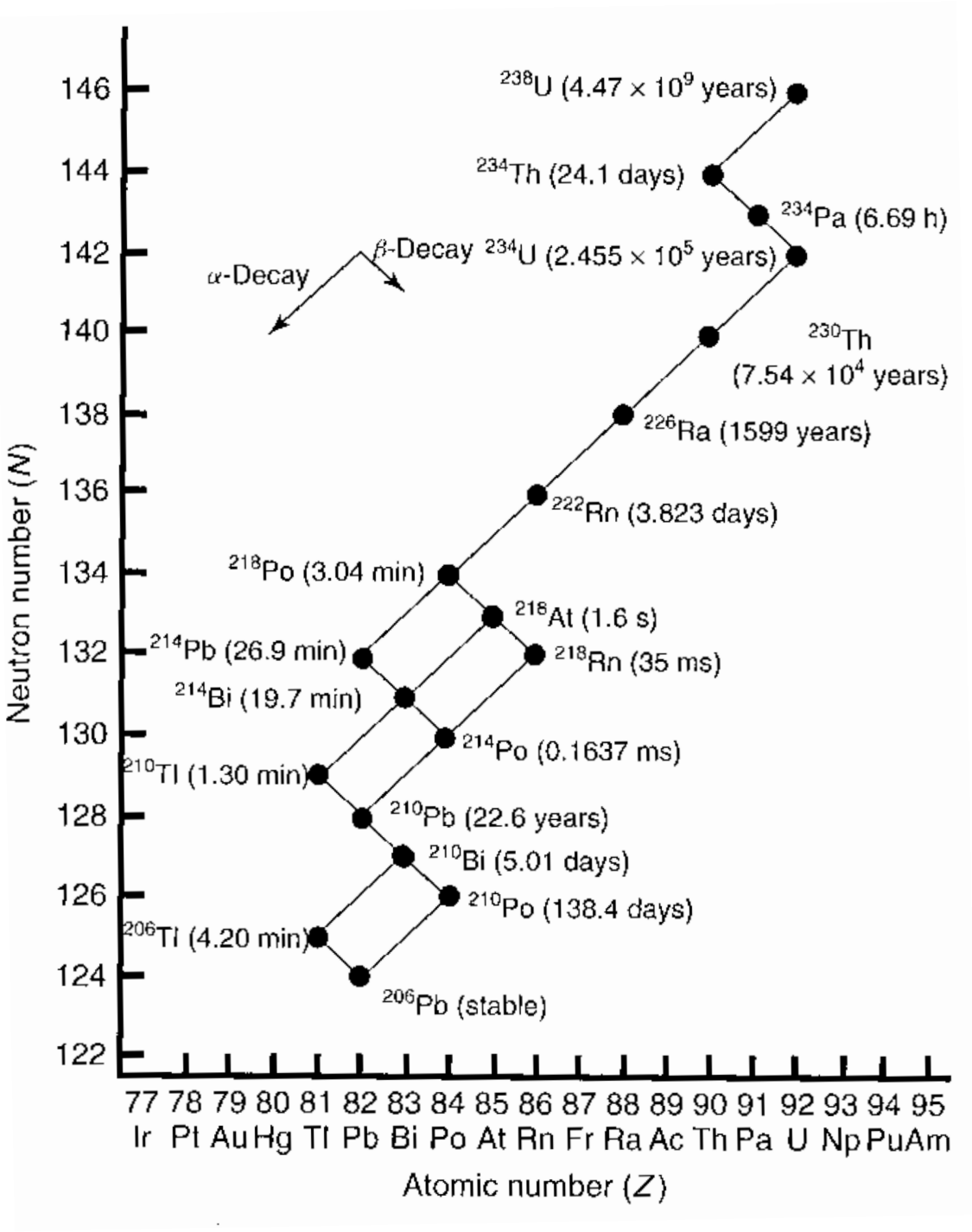

U-238: 12.35e3 Bq
Th-234: 12.35e3 Bq
Pa-234m: 12.32e3 Bq
U-234: 12.35e3 Bq
Th-230: 1.111 Bq
Ra-226: 2.405e-3 Bq
Rn-222: 2.397e-3 Bq
Po-218: 2.397e-3 Bq
Pb-214: 2.397e-3 Bq
Bi-214: 2.397e-3 Bq
Po-214: 2.397e-3 Bq
Pb-210: 229.9e-6 Bq
Bi-210: 228.6e-6 Bq
Po-210: 195.6e-6 Bq
At-218: 479.5e-9 Bq
Pa-234: 40.73 Bq

U-235: 568.7 Bq
Th-231: 568.7 Bq
Pa-231: 120.2e-3 Bq
Ac-227: 17.26e-3 Bq
Th-227: 16.78e-3 Bq
Ra-223: 16.87e-3 Bq
Rn-219: 16.87e-3 Bq
Po-215: 16.87e-3 Bq
Pb-211: 16.87e-3 Bq
Bi-211: 16.87e-3 Bq
Tl-207: 16.82e-3 Bq
Po-211: 47.25e-6 Bq
Fr-223: 238.1e-6 Bq

Total activities after 10 years:
U-238 Series: 49.43e3 Bq
U-235 Series: 1.137e3 Bq

Grand Total: 50.56e3 Bq

Input = 1g

Natural uranium (238 + 235) : Activities after 10 years:

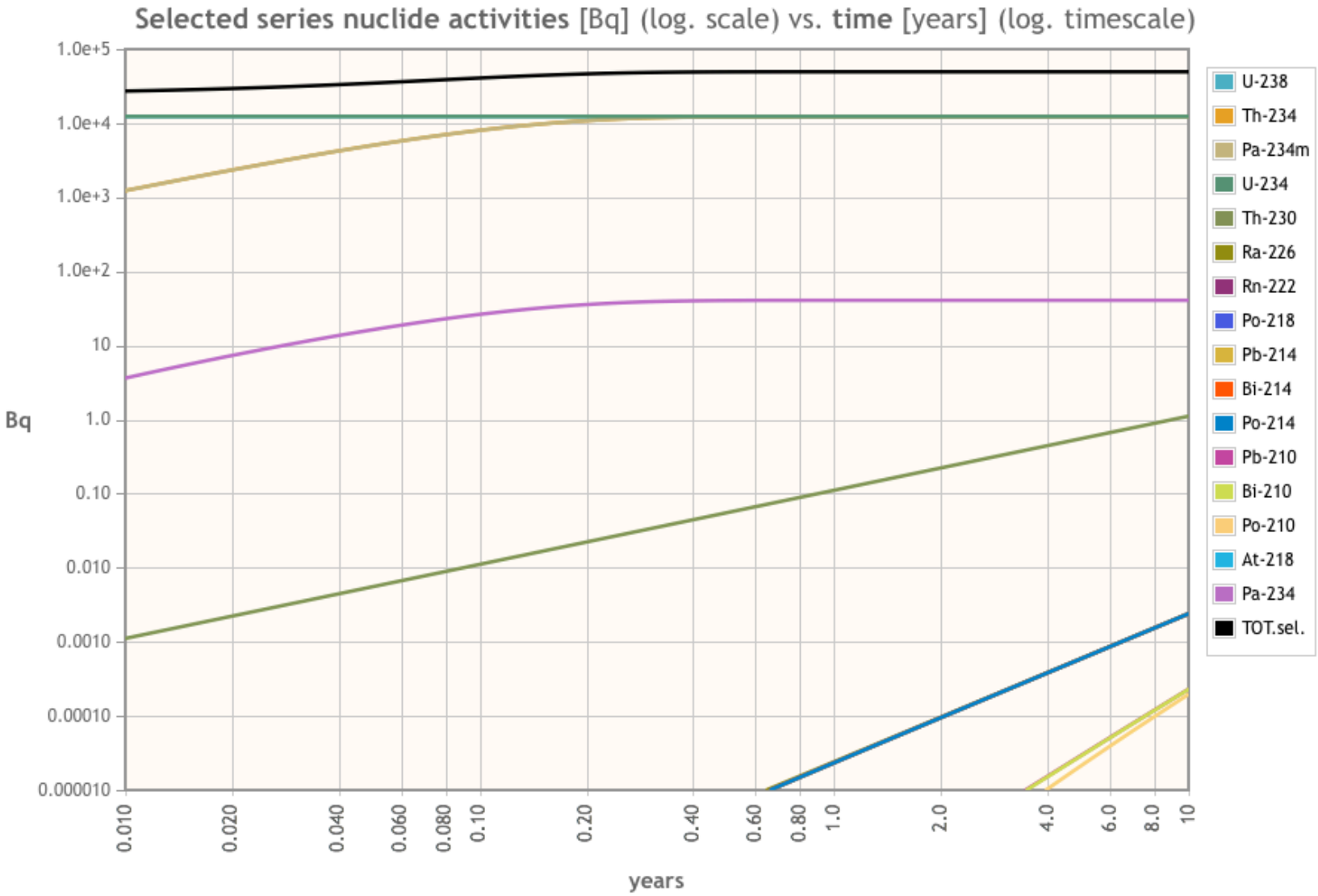

http://www.wise-uranium.org/rccu.html

1.3 Anthropogenic radioactivity in the atmosphere

Anthorpogenic radioactivity : radioactive substances that did not exist on earth before the nuclear era

The first injection of plutonium into the atmosphere occurred in July 16th 1945 with the detonation of the first plutonium device at the “Trinity Site” near Alamogordo in New Mexico, USA.

Last atmospheric test : China October 18th 1980

The Trinity Test took place at 5:29:45 a.m. Mountain War Time on July 16, 1945. These photographs of the Trinity Test were taken at 10,000 yards north made by an 18" Mitchell camera running at 120 frames per second (fps). Times given are approximate. Photographer: B. Brixner. (.006 second / Neg. TR018_1A)

543 nuclear weapons tests were conducted worldwide in the atmosphere between 1945 and 1980.

Approximately 6.52 PBq (1 Peta Bq = 10^{15} Bq) of 239Pu, 5.35 PBq of 240Pu, and 142 PBq of 241Pu were released into the atmosphere from nuclear weapons testing

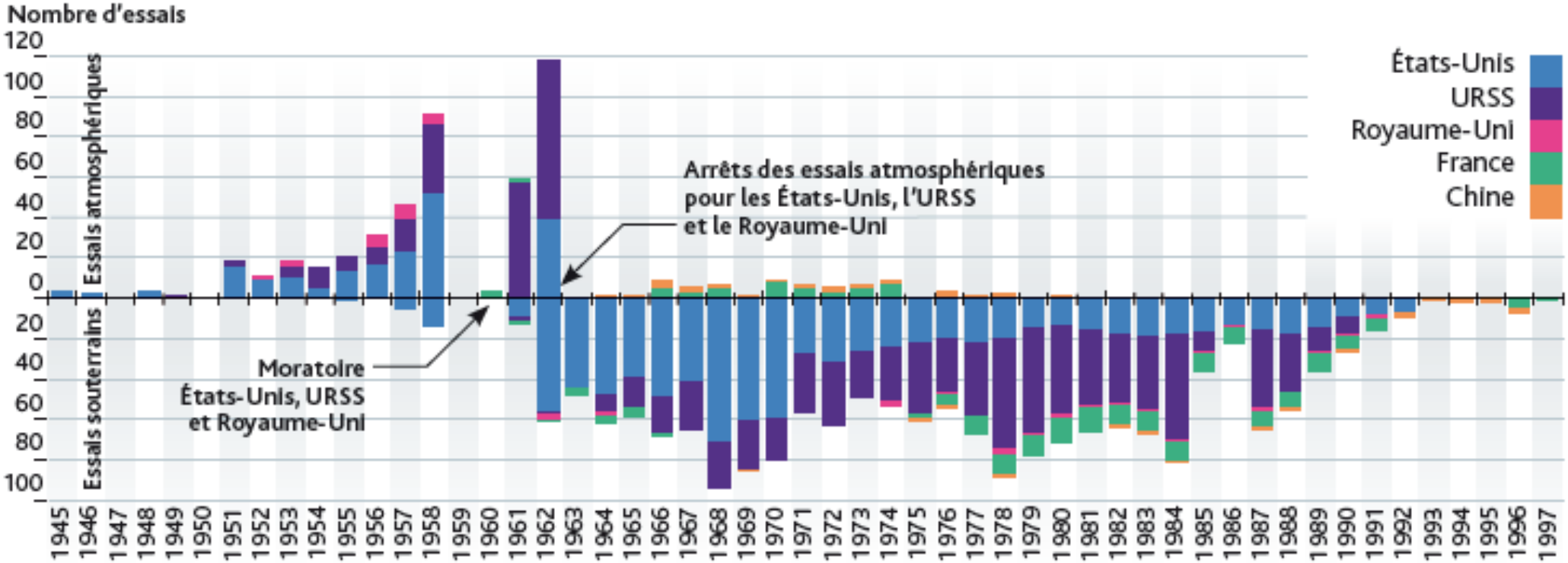

IRSN, fiche "les retombées en France des essais nucléaires atmosphériques"
Journal of Environmental Radioactivity 175-176 (2017) 39

Power of the atmospheric tests

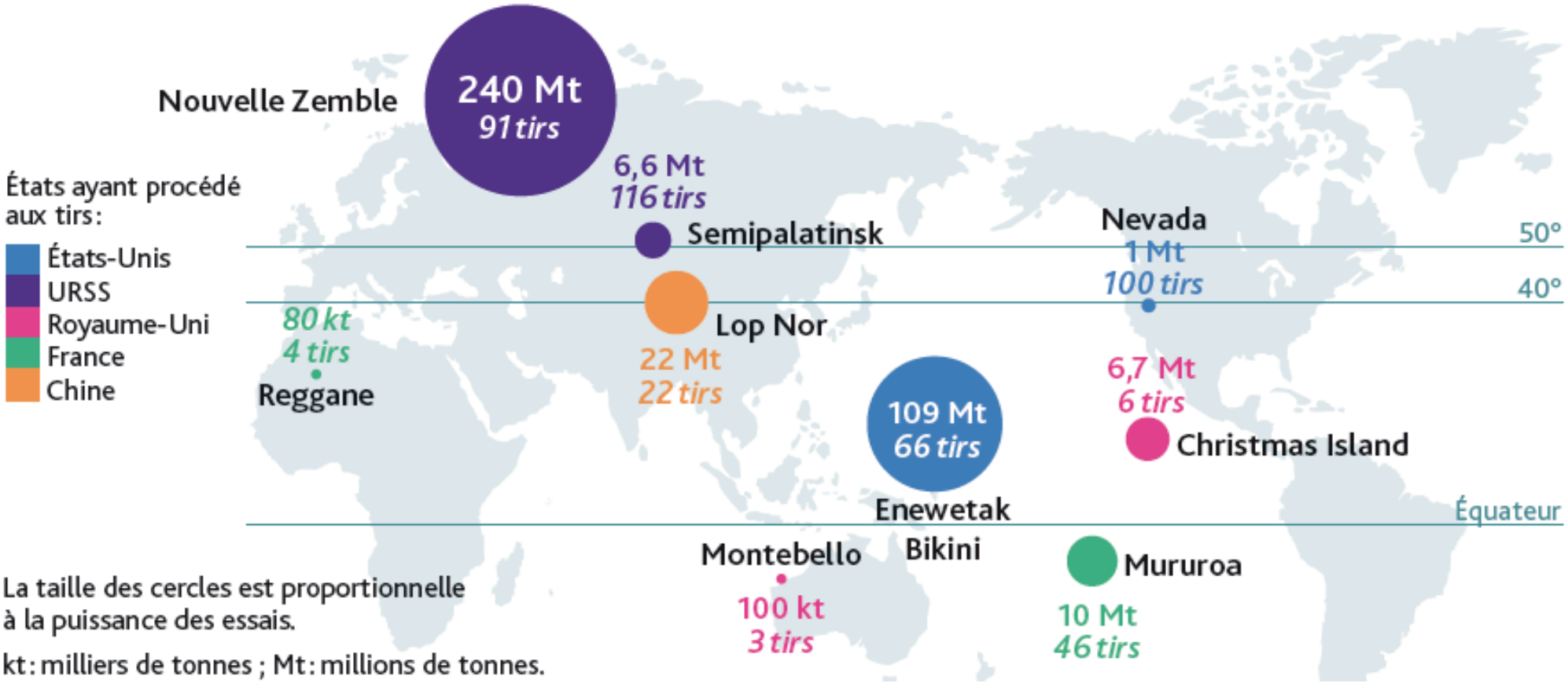

Comparison : Hiroshima and Nagasaki, 20 kT each
France represents 2.3% of the total power

Source : IRSN, fiche “les retombées en France des essais nucléaires atmosphériques”

Mushroom head
- 20 kt -> troposphere – stratosphere limit
- 150 kt -> ≈ stratosphere
- > 1 Mt -> over 25 km

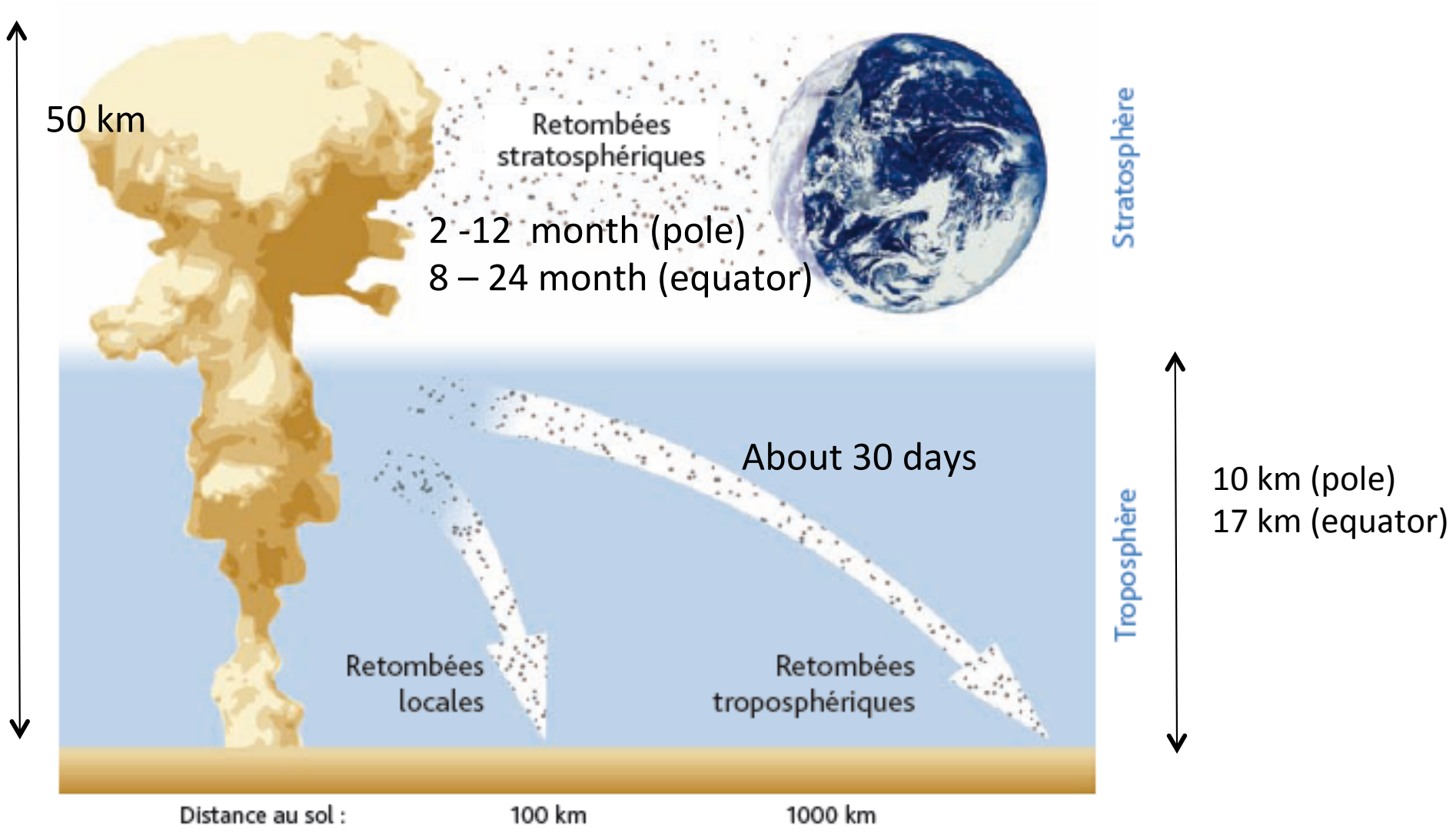

Source : IRSN, fiche “les retombées en France des essais nucléaires atmosphériques”

Sources of fallout : survey

✔ The largest source of **stratospheric** fallout, which peaked in 1962, is characterized by a 240-Pu/239-Pu atom ratio of 0.18

✔ The second source is **tropospheric** fallout with a lower 240-Pu/239-Pu ratio of 0.035 and is proposed to be originated from surface-based low yield testing at the Nevada Test Site

✔ Two other sources of fallout :

- The **Chernobyl accident** (April 1986) increased the concentration of 239+240Pu in surface air during 1986-1987 (6.1 PBq of plutonium isotopes), especially in Europe and contributed to the plutonium global inventory with a 240-Pu/239-Pu atom ratio of ~0.40
- The high altitude destruction of the **SNAP-9A satellite** power source over the South Pacific in 1964 contributed about 0.6 PBq of 238-Pu to the global inventory

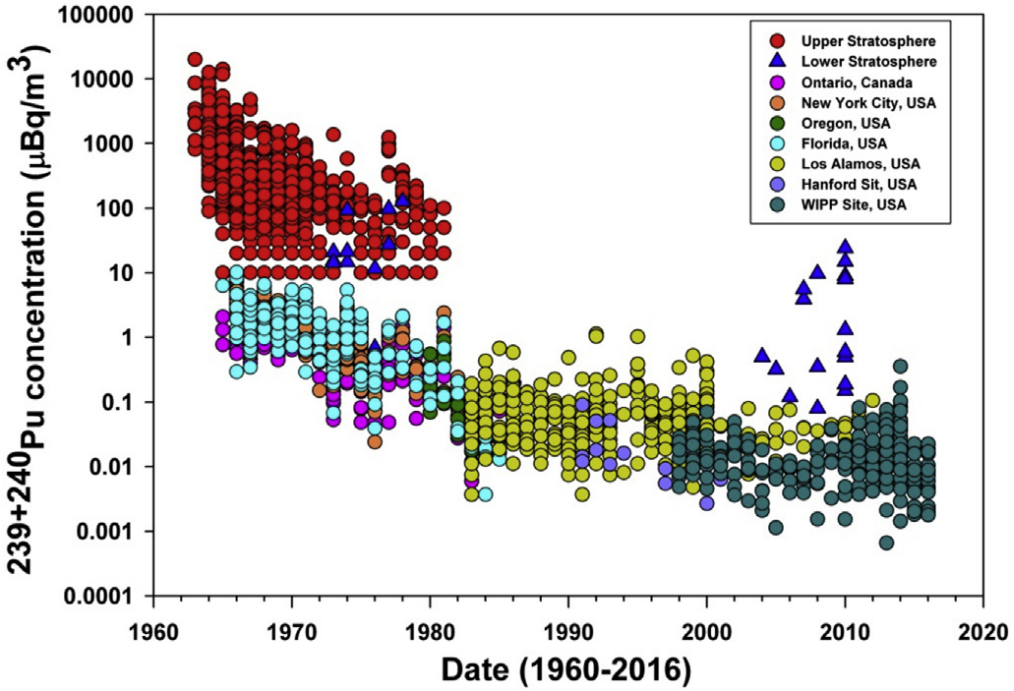

Temporal variations of 239+240-Pu concentrations (mBq/m3) in stratosphere and surface air in the Northern Hemisphere.

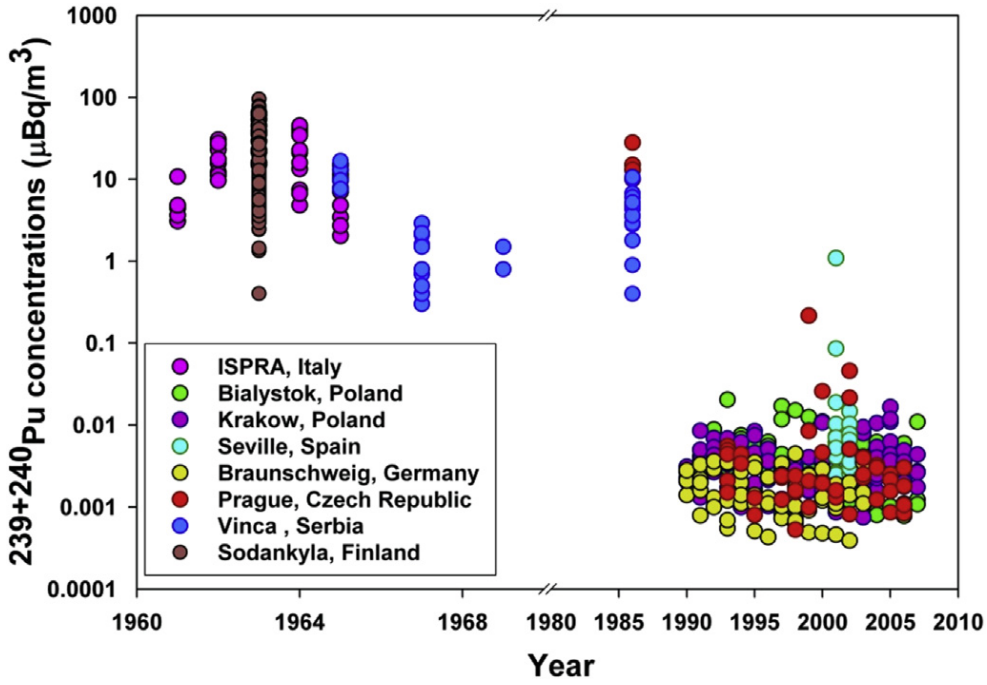

Temporal variations of 239+240-Pu concentrations (mBq/m3) in surface air in the Europe.

✔ It is therefore generally accepted that the current level of plutonium in the stratosphere is negligible and that most of plutonium in the air today is associated with resuspended soil, which is contaminated from nuclear weapons testing fallout.

=> global dust storms and biomass burning/wildfire also play an important role in redistributing plutonium in the post fallout air.

Journal of Environmental Radioactivity 175-176 (2017) 39

1.4 Oceans and seas

	Seawater (mM)	Lakes (mM)
Cl^-	535	0,054 à 0,68
SO_4^{2-}	9 à 28	0,03 – 0,53
HCO_3^-	2,3	0,31 – 1,85
Br^-	0,84	-
F^-	0,068	0,011 à 0,016
SiO_2	0,11	0,12 – 0,17
B	0,42	-
Na^+	465	-
Mg^{2+}	52,7	0,045 – 0,41
Ca^{2+}	10,0	0,11 – 0,95
K^+	9,7	0,033 – 0,074
Sr^{2+}	0,15	-

Covers about 70.8 % of the earth surface

Average salinity = 35 g / kg (from 10 to 40 g / kg)
Average pH = 8.2 (from 7.4 to 8.4)
Ionic strength = 0.6 - 0.7 M
E = 210 mV

Major sources of radionuclides :

- testing of nuclear weapons in the atmosphere
- undewater island tests
- discharge from nuclear fuel reporcessing plants
- accident of SNAP-9A satellite
- submarine accidents (Thresher in 1963, Komsomolet in 1989)
- Tchernobyl (April 1986) and Fukushima (March 2011) accidents
- natural radioactivity, essentially primordial (40-K, 238-U, 235-U and 232-Th)

Actinide	Concentrations typiques (M)	Concentrations en Méditerranée (M)
^{232}Th	$4{,}3.10^{-13}$	$< 3.10^{-12}$
$^{234,238}U$	$1{,}3.10^{-8}$	$^{238}U = 1{,}4$ à $1{,}6.10^{-8}$
^{238}Pu	3.10^{-18}	
^{239}Pu	1.10^{-14}	$^{239,240}Pu \approx 1.10^{-17}$
^{240}Pu	3.10^{-15}	
^{241}Pu	8.10^{-17}	
^{241}Am	4.10^{-17}	5.10^{-20} à 1.10^{-19}
^{237}Np	2.10^{-14}	
^{90}Sr	$4{,}3.10^{-15}$	
^{137}Cs	4 à 7.10^{-18}	$5{,}7.10^{-18}$

Average concentrations of radionuclides in seawater

Marine Chemistry (1989) , 28, 19
Science of The Total Environment (1989) 83(3), 203

137-Cs fallout

Global 137-Cs fallout are in adjacent regions.

- Kuroshio at the latitude of 20–401 N in the Pacific Ocean
- Gulf Stream areas at the latitude of 30–501 N in the Atlantic Ocean.

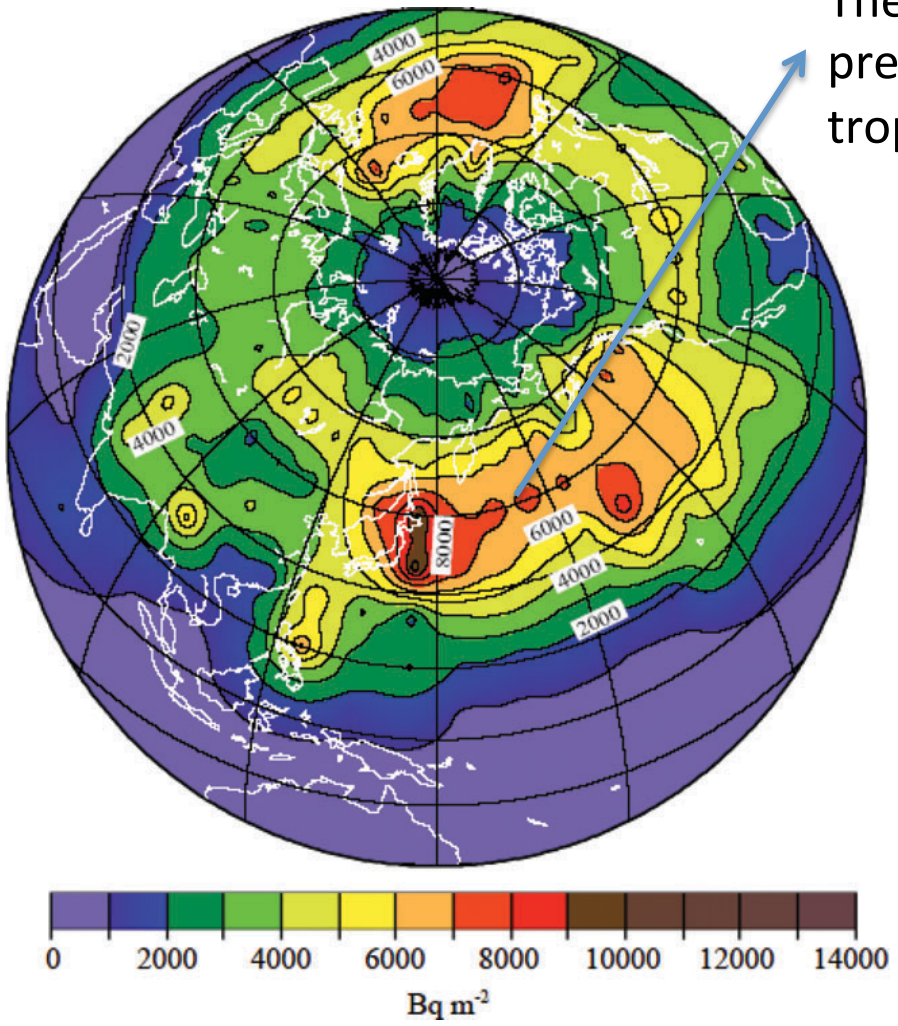

These regions are crossroad of larger precipitation region and higher stratosphere–troposphere exchange region.

Table 1 Summary of global ^{137}Cs deposition in the form of the UNSCEAR model

Latitude/°	Average/ Bq m^{-2}	Integral/ PBq	Range/ Bq m^{-2}	UNSCEAR/ Bq m^{-2}
Northern hemisphere				
85	900	3.5	820–990	280
75	1970	22.8	880–5280	800
65	3420	64.5	1110–8060	2050
55	5040	128.9	2770–7910	3430
45	5090	159.8	1540–10230	3830
35	4100	149.0	700–10630	2780
25	2620	105.0	120–6430	2110
15	1820	77.6	380–7280	1420
5	1300	57.3	410–3860	970
Southern hemisphere				
−5	800	35.1	100–1210	510
−15	530	22.8	120–1060	440
−25	470	18.7	170–830	750
−35	580	21.1	150–1430	810
−45	NA			
−55	NA			
−65	NA			
−75	NA			
−85	NA			

Re-constructed global 137-Cs fallout as of 1 January, 1970 (Bq m^{-2}).

J. Environ. Monit (2006), 8, 431.

2. Uranium, Neptunium and plutonium chemistry in the environment

2.1 General trends

Depends on the oxidation state

General trend of the actinide complexes : $An^{4+} > AnO_2^{2+} > An^{3+} > AnO_2^{+}$

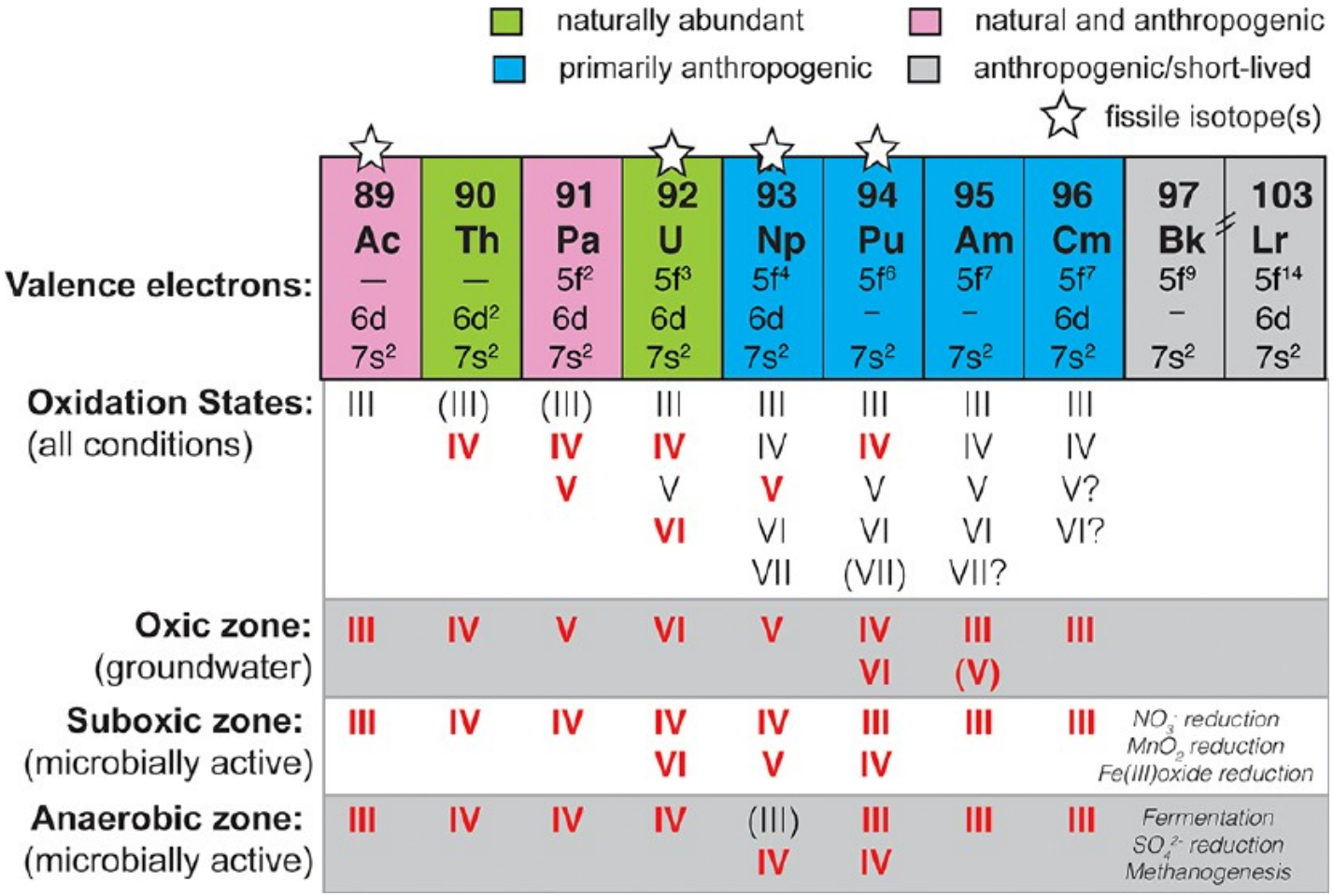

Inorg. Chem. (2013) 52, 3510

✔ RedOx and speciation can be modified by :

- the Eh of the medium (water)
- the ligand containt (carbonate, silicate, phosphate)
- the microbial activity
- sorption processes

=> Thermodynamic, kinetic and biological processes

✔ Because of their ubiquity in natural waters, **hydroxide** and **carbonate** are the most important ligands for actinide complexation (specially for An(IV)).

✔ Key differences among U, Pu, and Np speciation.
Plutonium has the most complex redox chemistry of the actinides, with multiple valence states (III to VI) stable under typical pH and redox conditions of subsurface environments.

✔ The chemistry of pentavalent actinides is chiefly governed by the disproportionation reaction.

$$2AnO_2^+ + 4H^+ \rightarrow An^{4+} + AnO_2^{2+} + 2H_2O$$

V -> IV + VI

2.2. Pourbaix diagrams, U, Np, Pu

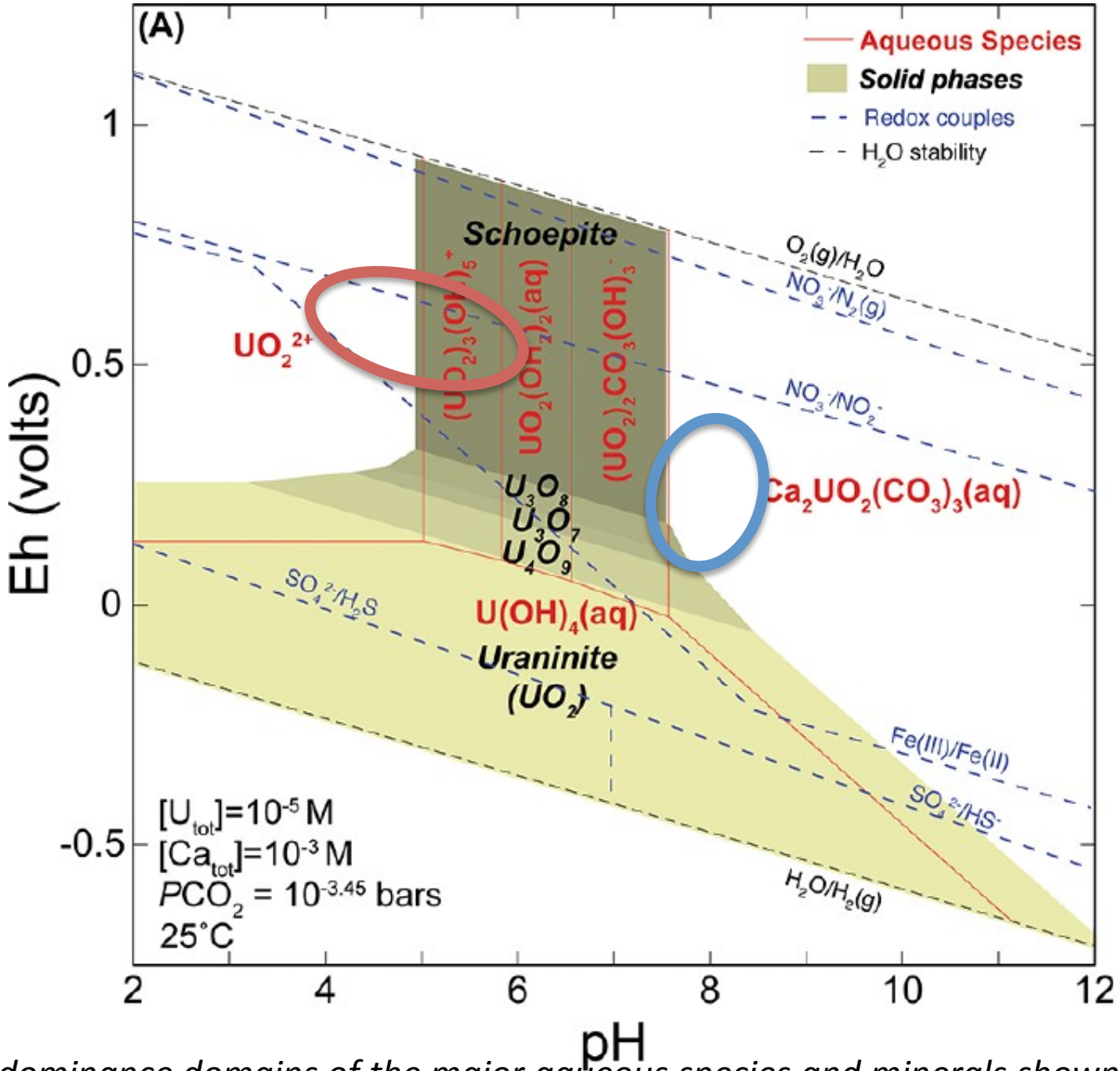

Surface water

Seawater

Inorg. Chem. (2013) 52, 3510

Predominance domains of the major aqueous species and minerals shown as a function of the Eh (V) and pH for total uranium [UTot] = 10^{-5} M in water containing calcium ions ([CaTot] = 10^{-3} M) and in equilibrium with atmospheric CO_2 (P_{CO2} = 10−3.45 bars). Dashed lines define the environmentally relevant redox couples

✔ Oxidized hexavalent uranium is highly soluble as the uranyl ion UO_2^{2+}, whereas the solubility of U^{4+} is largely controlled by insoluble oxides such as uraninite UO_2

✔ Hydrolysis of the uranyl ion becomes important above pH ~4, where hydroxo complexes compete with other inorganic and organic ligands in solution, including carbonate, phosphate, sulfate, silicate, and n-carboxylic and humic acids

(a) $AnO_2(CO_3)^{m-2}$ (b) $AnO_2(CO_3)_2^{m-4}$ (c) $AnO_2(CO_3)_3^{m-6}$

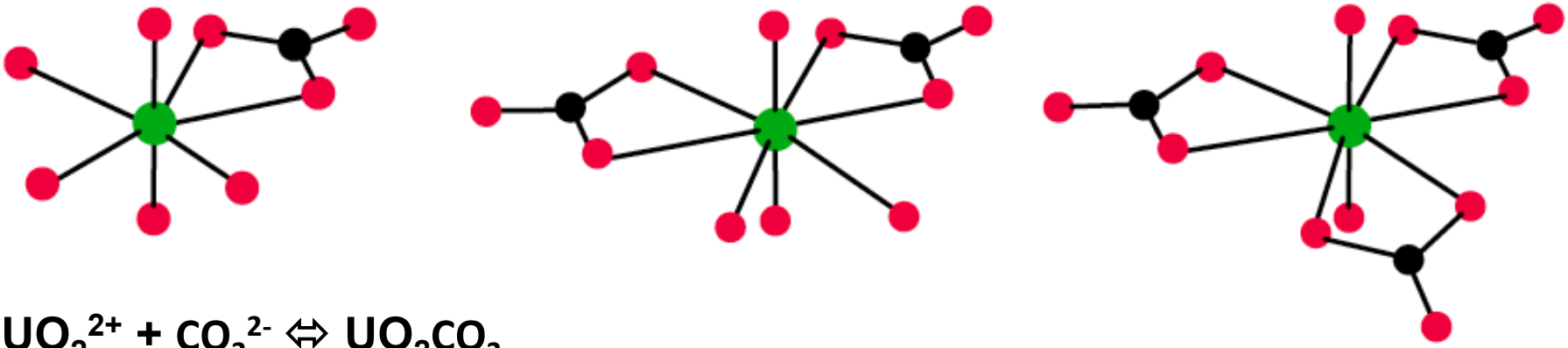

$$UO_2^{2+} + CO_3^{2-} \Leftrightarrow UO_2CO_3$$

$$UO_2CO_3 + CO_3^{2-} \Leftrightarrow UO_2(CO_3)_2^{2-}$$

$$UO_2(CO_3)_2^{2-} + CO_3^{2-} + 4\,NH_4^{+} \Leftrightarrow (NH_4)_4UO_2(CO_3)_3$$

W. Runde *et al. Los Alamos Science* (2000), **26**, 393.

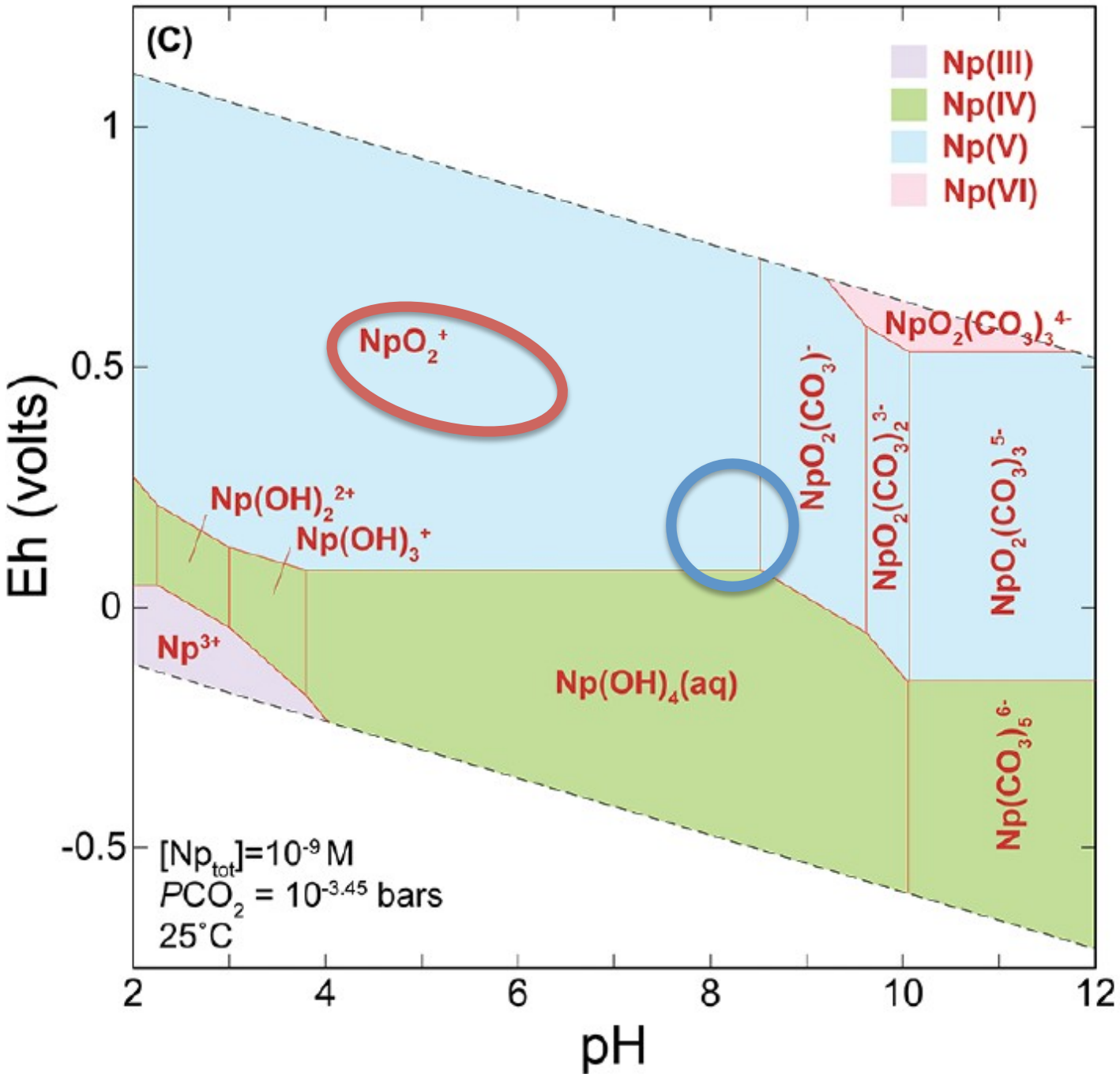

Surface water

Seawater

Inorg. Chem. (2013) 52, 3510

Neptunium speciation with oxidation states represented in colors as in part B. Diagrams are calculated using the Geochemist's Workbench and the LLNL V8 R6 "combined" database.

✔ Neptunium is stable under oxic to moderately suboxic conditions as the trans-dioxoneptunyl cation NpO_2^+ or as neptunylcarbonato complexes at high pH

=> neptunium (neptunyl) is generally the most soluble and mobile of the actinides

✔ Np^{4+} is favored in anoxic environments and hydrolyzes to form polymeric hyroxides, similar to Pu(IV).

✔ Although NpO_2 is thermodynamically favored, it has not been identified in solubility experiments involving natural waters / only amorphous Np(IV) solid phases precipitated

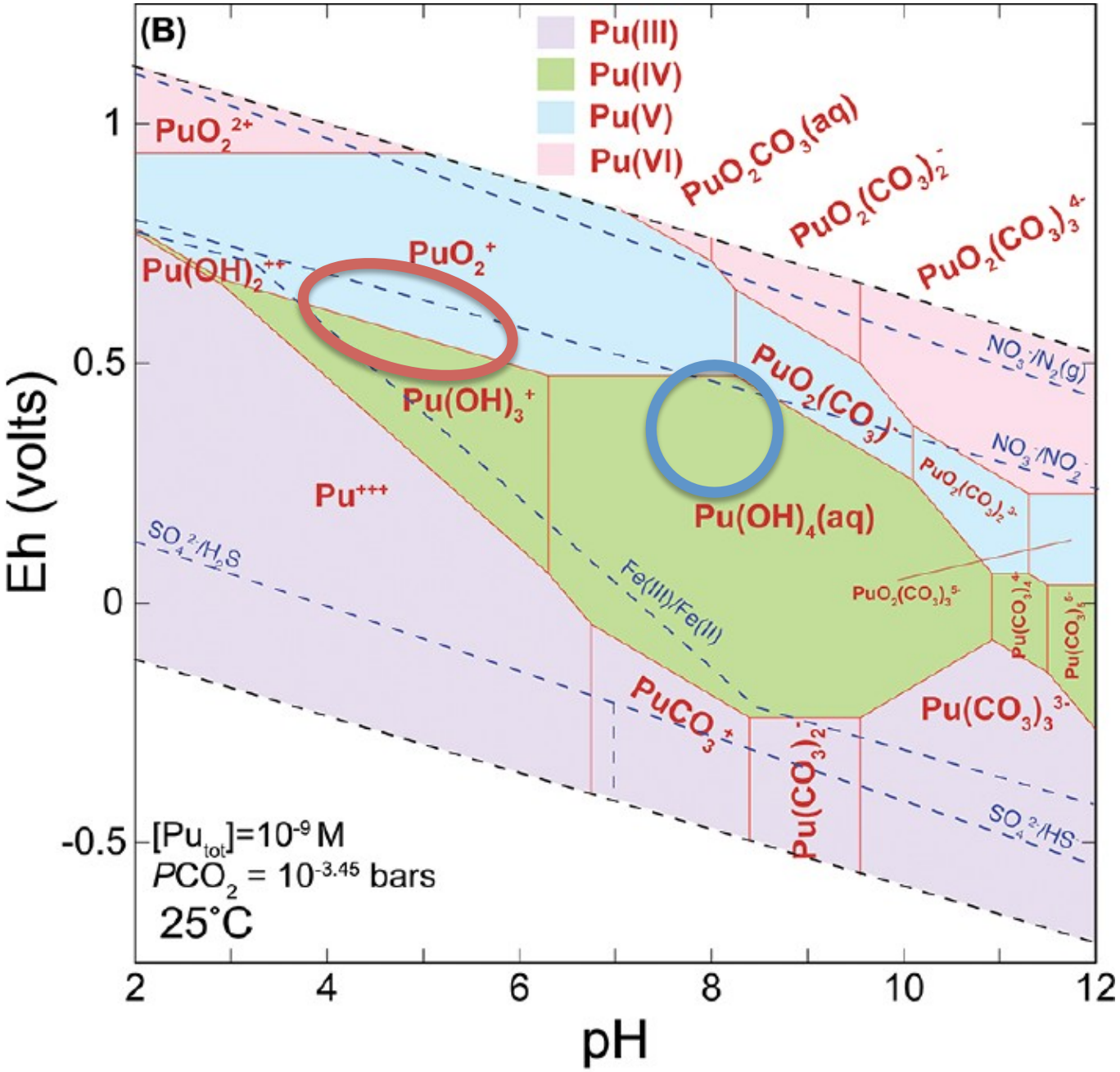

Plutonium speciation where colors represent the different oxidation states and the corresponding aqueous speciation

Surface water

Seawater

E (V)

PuO_2^{+}	Pu^{4+} 1.04 V
Pu^{4+}	Pu^{3+} 1.01 V
PuO_2^{2+}	Pu^{4+} 0.99 V
PuO_2^{2+}	PuO_2^{+} 0.94 V

Inorg. Chem. (2013) 52, 3510

✔ General trends :

- Disproportionation of Pu^{4+} and PuO_2^{+}
- PuO_2^{+} and PuO_2^{2+} predominate under oxic conditions
- Pu^{4+} is most common in neutral pH

✔ In the tetravalent state, the aggregation of hydrolysis products ($[Pu(OH)_n]^{(4-n)+}$) results in the formation of hydroxo-bridged polymers.

✔ If crystalline $PuO_2(s)$ is considered the dominant control on plutonium solubility, the concentration of Pu^{4+} would be ~10^{-17} M

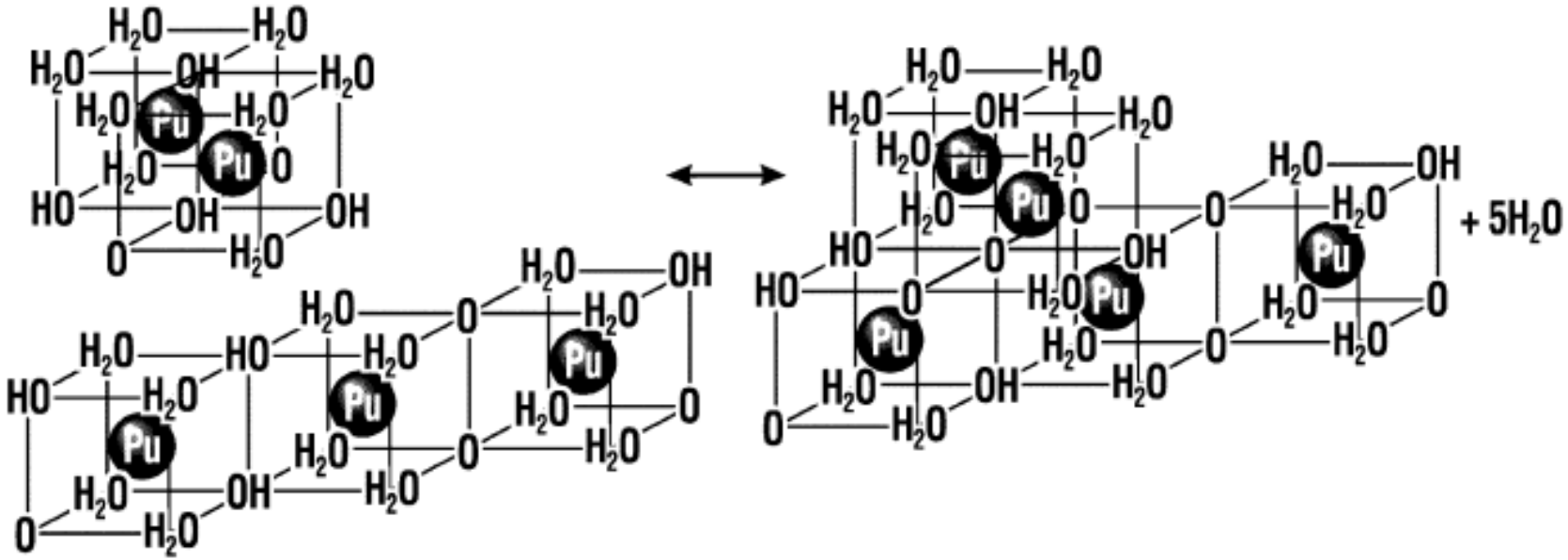

Importance of the carbonate ions to stabilize the +V and +VI oxidation states

Interaction strength :CO_2 > $C_2O_4^{2-}$ > HPO_4^{2-} >SO_4^{2-}

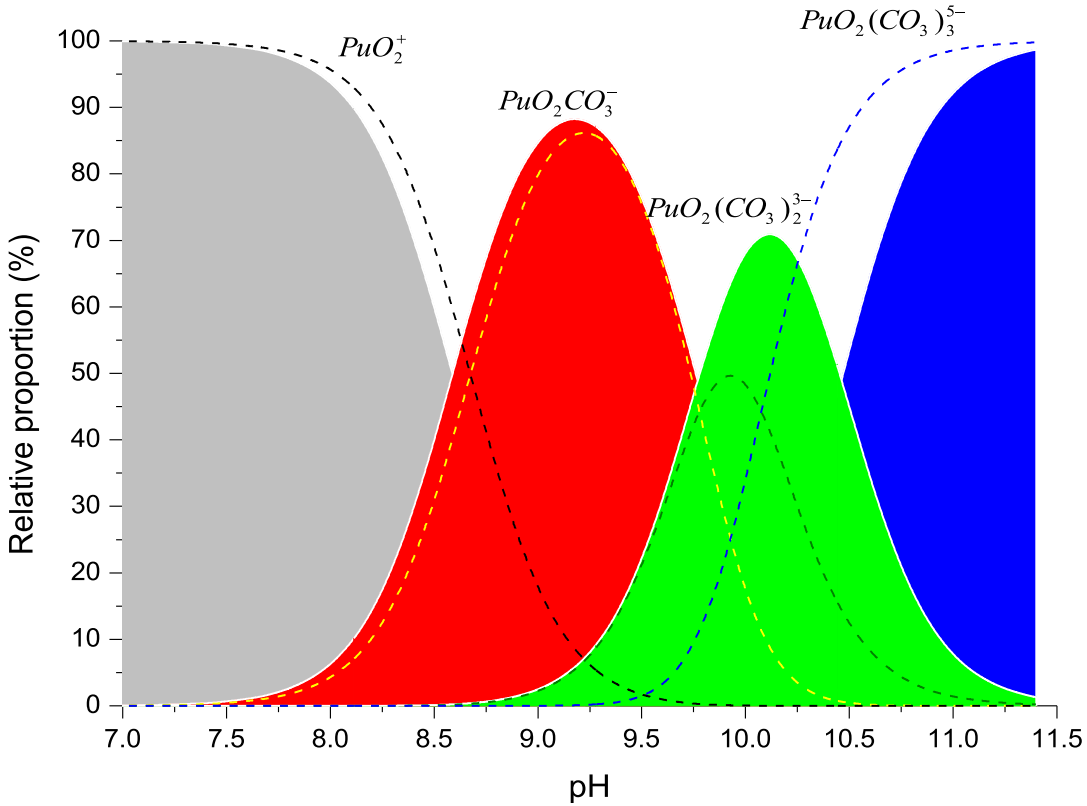

Np(V) – Pu(V) analogy :
Pu bond length, for Pu(V), is slightly smaller than that of Np(V)

-> higher charge density, and stronger interaction with carbonate ions.

Comparison of the Pu(V)/carbonate ions speciation diagram, using data from NEA (filled-in areas) and from CEeICPeMS (dashed lines) with PuO_2^+ , $PuO_2(CO2)3$, $PuO_2(CO_3)_23$-, $PuO_2(CO_3)_3^{5-}$.Conditions: I = 1=0.60mol/L, Pco2 =310^{-4} bar,T=25±1C.

Journal of Environmental Radioactivity 153 (2016) 237

2.2 Hydrolysis

Most important reaction in natural environment

$$xM^{z+} + yH_2O \Leftrightarrow M_x(OH)_y^{(xz-y)} + yH^+$$

$\log^*\beta°$ for the first and second hydrolysis reactions of An(IV) $\quad {}^*\beta° = \dfrac{(M_x(OH)_y^{(xz-y)})(H^+)^y}{(M^{z+})^x a_w^y}$

a_w = water activity = pH_2O/pH_2O^*, where pH2O is the water vapor pressure of the electrolyte solution and pH2O* is the value for pure water at the same temperature.

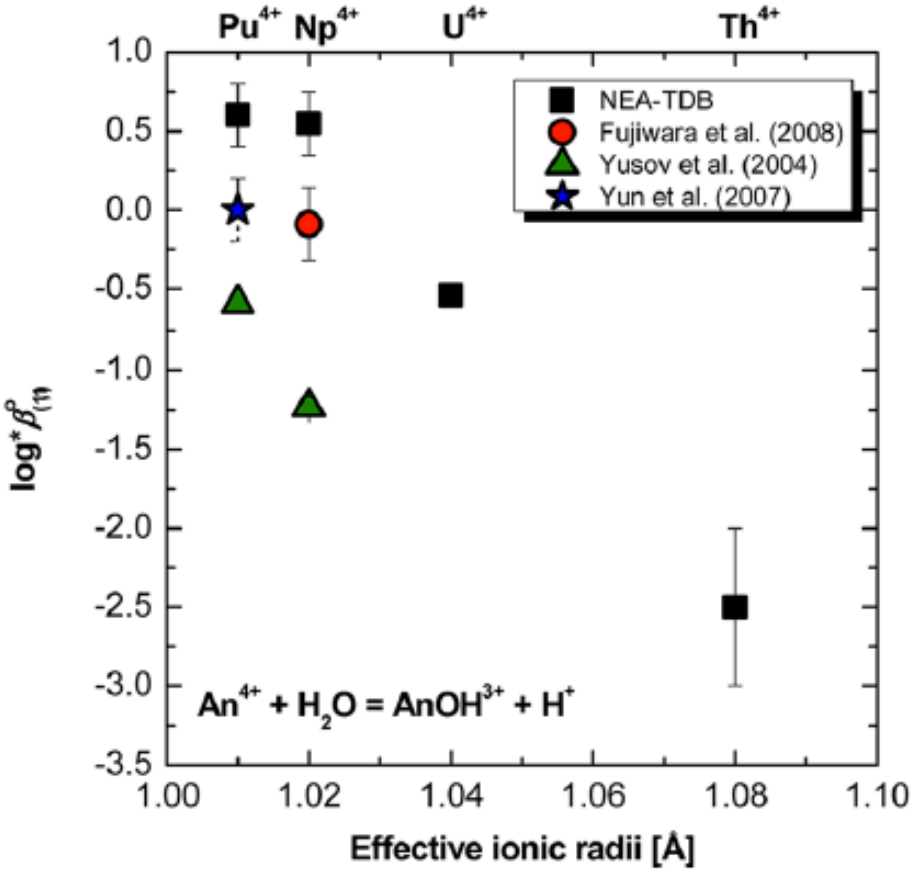

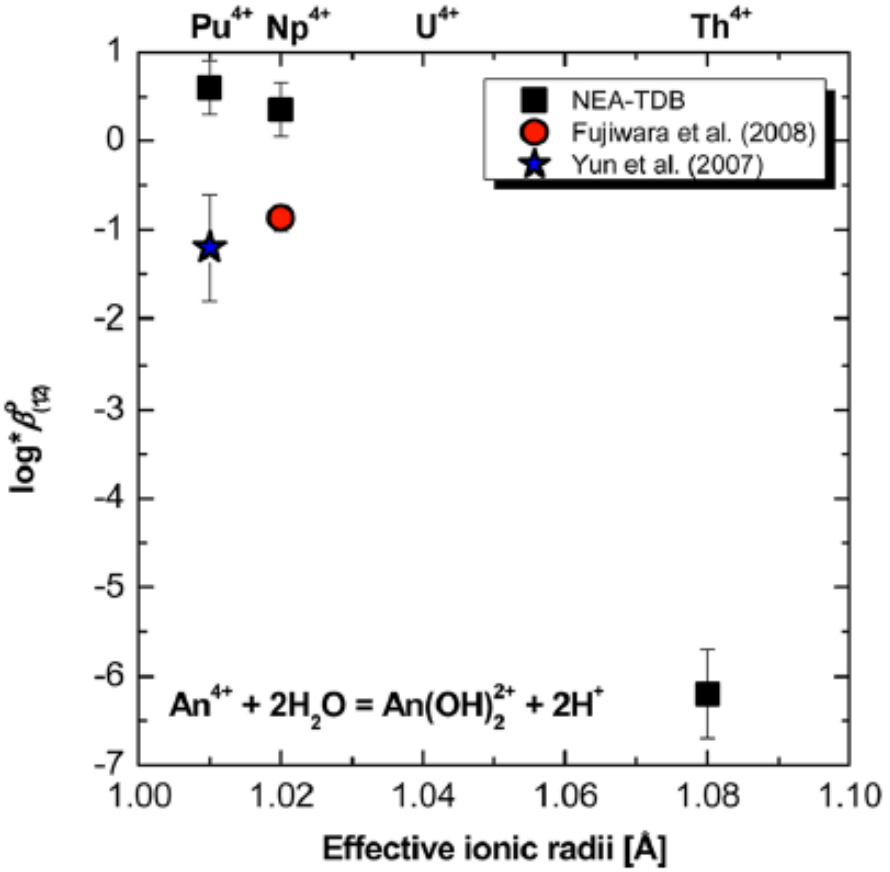

M. Altmaier, Chem. Rev. (2013), 113, 901

Controled hydrolysis

✔ Very large bibliography
dimers, trimers, tetramers, oligomers....

✔ Very often mixt structures with an excess of ligand.

✔ An(IV) are among the most acidic cations of the periodic table.

dioxydes (fluorite structure) Fm3m

AnO_2	An-O (Å)	An-An (Å)
ThO_2	2.424	3.958
PaO_2	2.384	3.893
UO_2	2.368	3.866
NpO_2	2.354	3.844
PuO_2	2.337	3.816
AmO_2	2.333	3.810

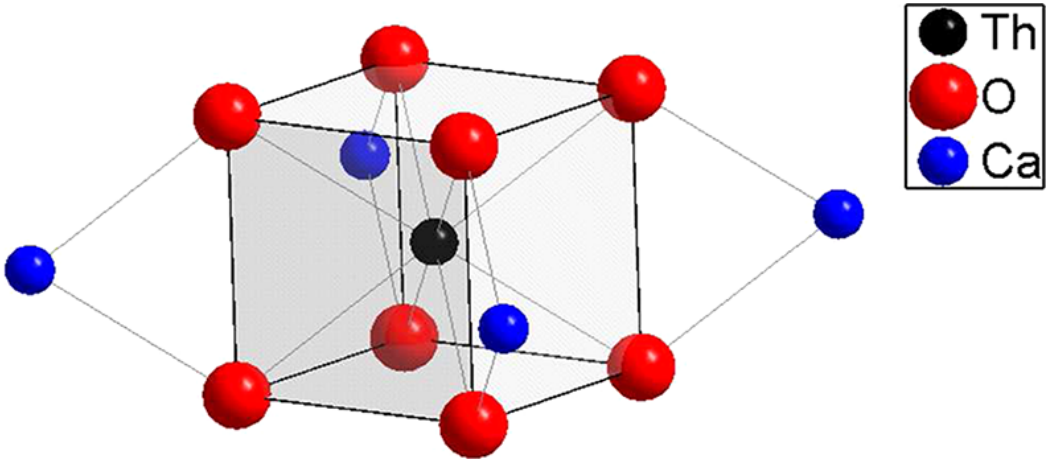

Idealized structure of the newly identified ternary complex Ca4[Th(OH)8]4+ with a distorted cubic structure.

Inorg. Chem. 2007, 46, 6804

Dimer of Th obtained after preicipation of Th nitrate with NH_4OH and washing of $Th(OH)_4$. Crysatalization in HCl 1M.

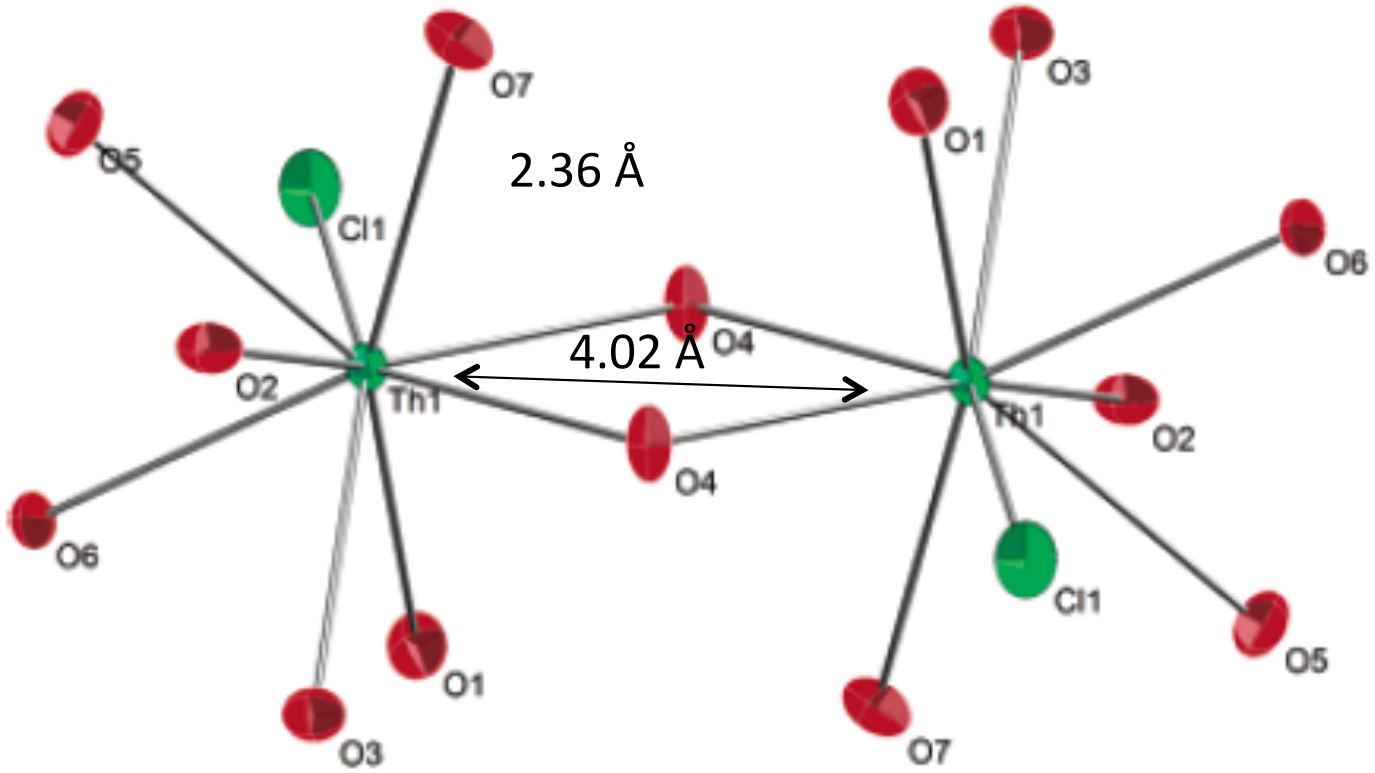

$[Th_2(\mu_2\text{-}OH)_2Cl_2(H_2O)_{12}]Cl_4.2H_2O$

Inorg. Chem. (2007), 46, 2369.

$[Co(NH_3)_6]_2[UO_2(OH)_4]_3.H_2O$

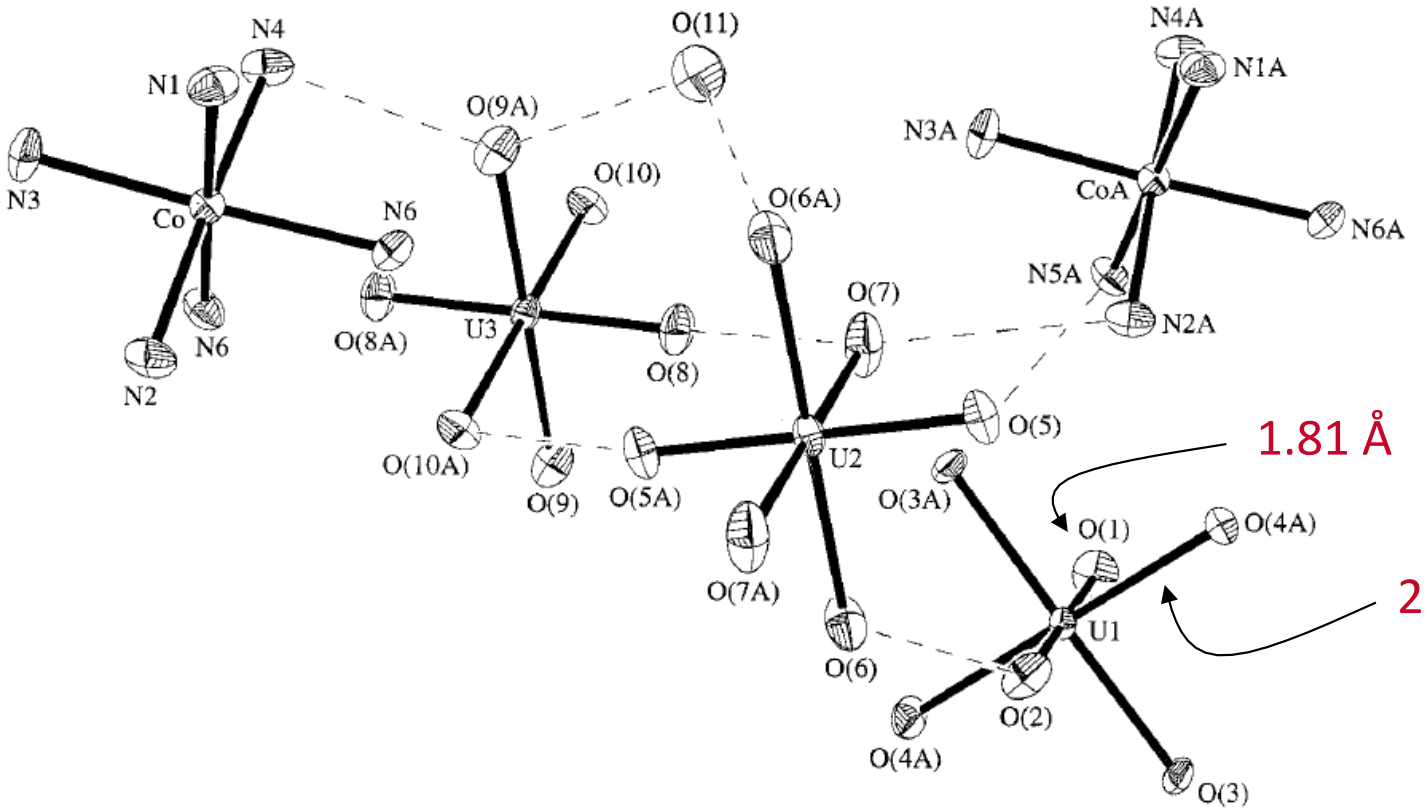

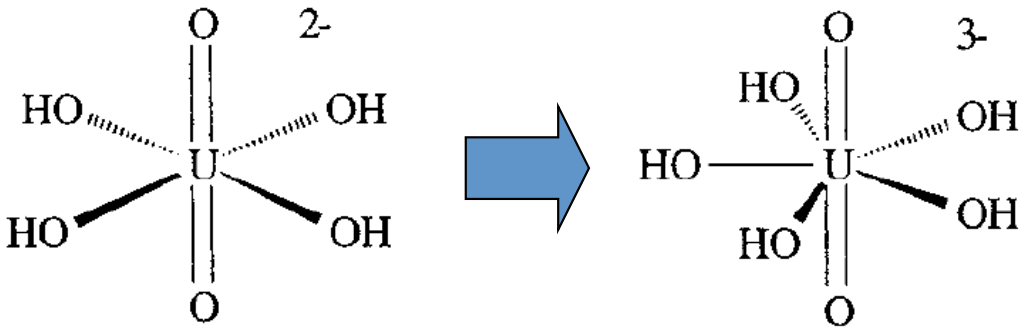

EXAFS structure

Solid state structure In solution (3.5 M TMAOH)

D. L. Clarck et al. Inorg. Chem. (1999), 38, 1456

$[Th_6(OH)_4O_4(H_2O)_6(Oac)_{12}].nH_2O$

Prepared from Th hydroxyde precipitate and subsequent dissolution in acetic acid

Hexanuclear core $[Th_6(OH)_4O_4]^{12+}$

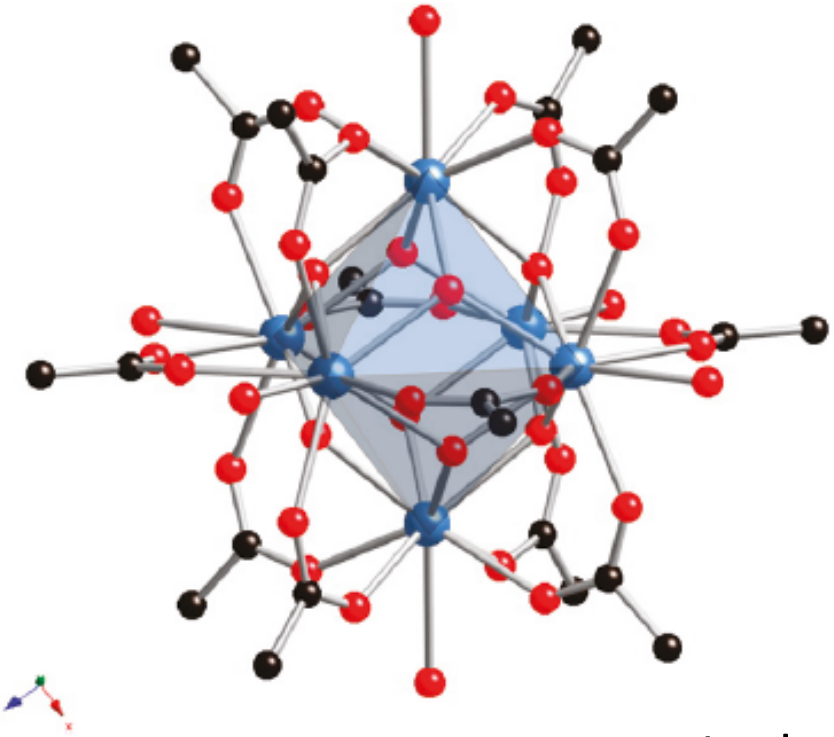

Th - μ_3-OH = 2.496 Å
Th - μ_3-O = 2.298 Å

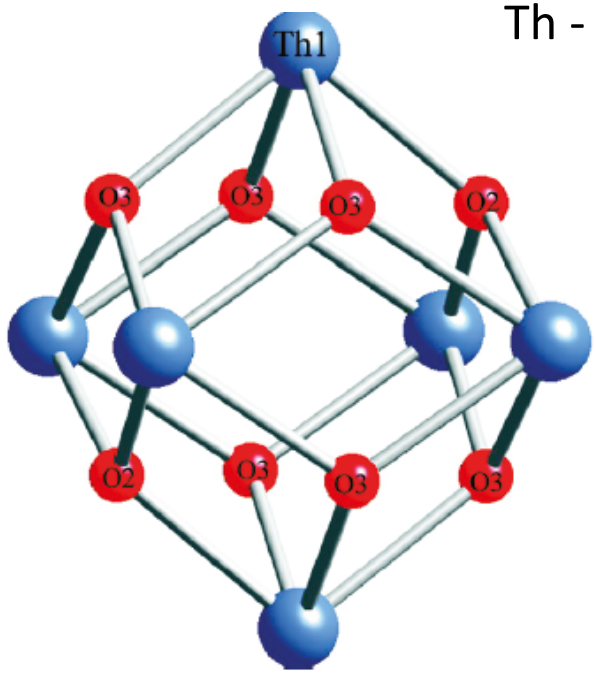

In the core
4 bridges μ_3-OH
4 bridges μ_3-O

Inorg. Chem. (2011), 50, 9696

Cluster of Pu_{38} in $Li_{14}(H_2O)_{20}[Pu_{38}O_{56}Cl_{54}(H_2O)_8]$

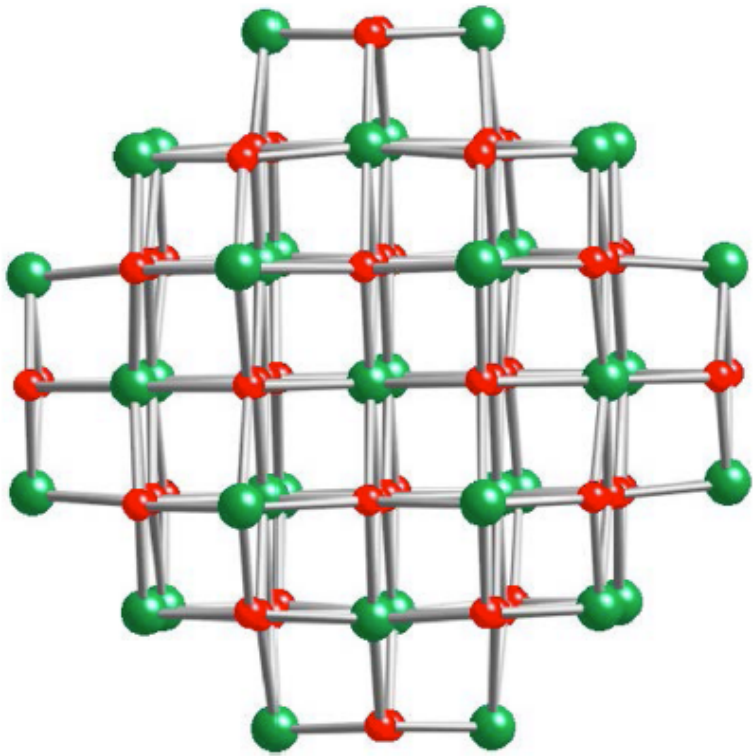

Illustration of the $[Pu_{38}O_{56}]^{40+}$ core observed in $Li_{14}(H_2O)_{20}[Pu_{38}O_{56}Cl_{54}(H_2O)_8]$ and $Li_2[Pu_{38}O_{56}Cl_{42}(H_2O)]\cdot 15H_2O$

Pu(IV) cations are bridged through exclusively oxo linkages into a structural topology that resembles that of bulk PuO_2.

Green and red spheres are Pu(IV) and O^{2-}, respectively.

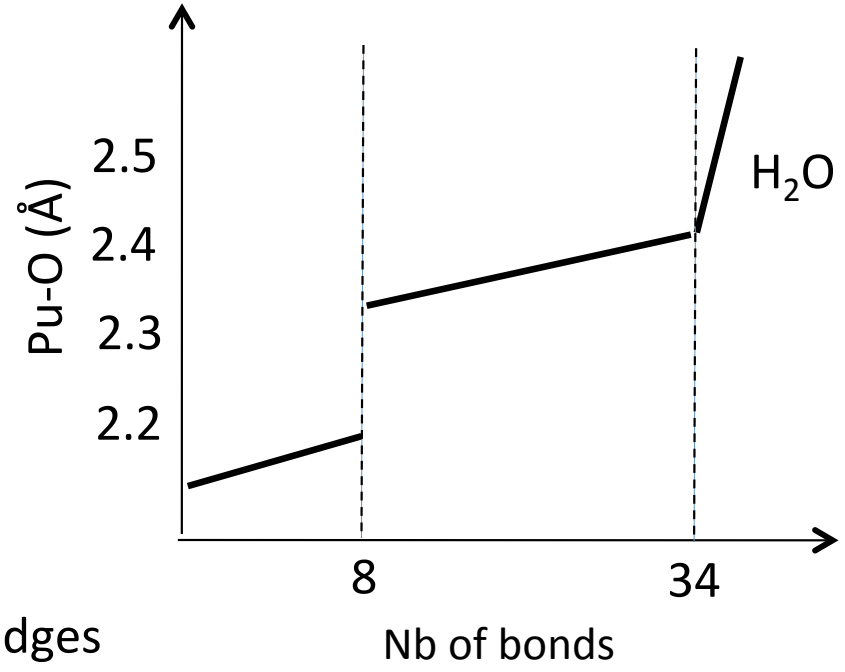

Core $[Pu_{38}O_{56}Cl_{54}(H_2O)_8]^{14-}$

No hydroxo bridges

C. Walther *et al. Chem. Rev*. (2013), **113**, 995
K. E. Knope et al. *Chem. Rev*. (2013), **113**, 944

2.3 Actinide minerals in NORM

NORM : Naturally Occuring Radioactive Materials

✔ One formation mechanism of actinide NORM nanoparticles occurring in nature is biomineralization/bioprecipitation of dissolved forms of uranium. Such microbial-mediated formed minerals are typically nanometer-sized and in hydrous phases, rendering them difficult to characterize in situ.

✔ Uraninite (UO_2) is both the dominant uranium ore mineral and the primary form of the fuel in light water reactors.

✔ The term uraninite is used to denote compositionally complex, nonstoichiometric, and generally cation-substi- tuted forms of UO_2 observed in nature

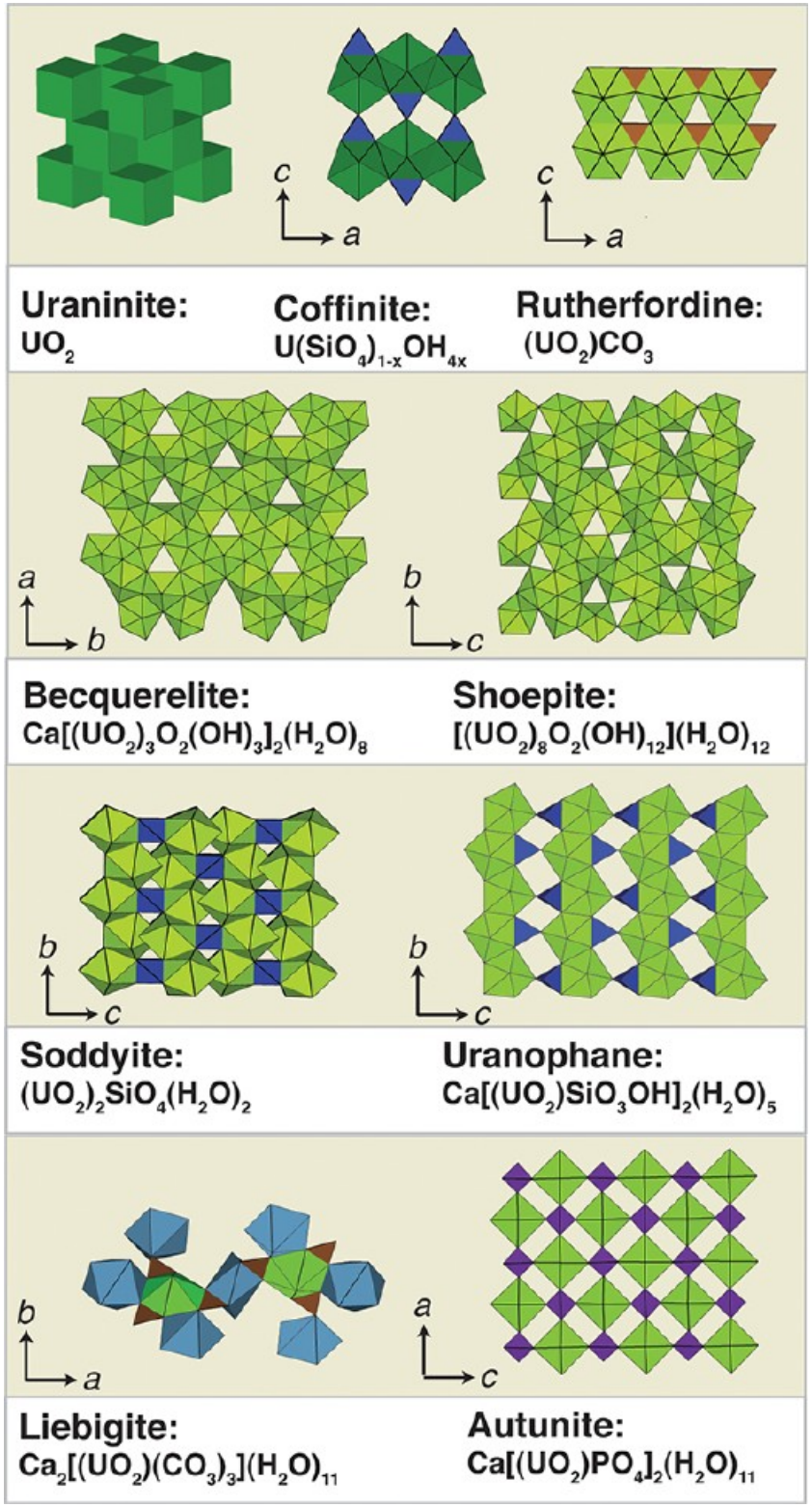

Common alteration of minerals includes :

- oxides and hydroxides such as
schoepite (UO3·1–2H2O)
becquerelite (Ca[(UO2)3O2(OH)3]2(H2O)8)

- carbonates like
rutherfordine (UO2CO3)
liebigite (Ca2UO2[(CO3)3]·11H2O)

- silicates like
uranophane (Ca- [(UO2)(SiO3OH)]2(H2O)5)
soddyite [(UO2)2SiO4·2H2O]

- phosphates such as
autunite (Ca- [UO2PO4]2·10–12H2O).

✔ Microbial U(VI) reduction has been shown to be catalyzed by many microorganisms, the majority being either metal- or sulfate-reducing bacteria

✔ Steps of biogenic uraninite formation

- Reduction of U(VI) to U(IV) by c-type cytochromes localized either in the periplasm or on the outer membrane
- Biogenic uraninite formation entails the precipitation of the mineral. It is generally believed that uraninite precipitates near the site of U(VI) reduction.

✔ The formation of uraninite by microbial U(VI) reduction was first demonstrated using the iron-reducing bacterium Geobacter metallireducens strain GS15

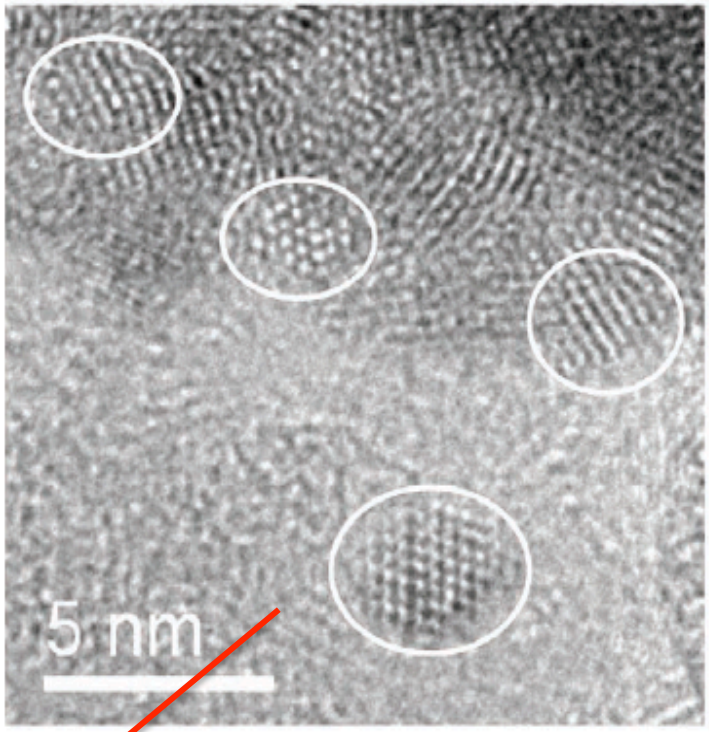

Fourier-filtered HR-TEM image of biogenic uraninite produced by Shewanella oneidensis strain MR-1, showing UO_2 lattice fringes.

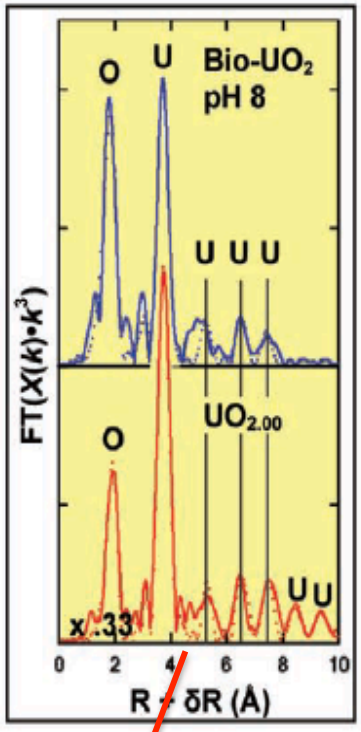

Fourier transforms (FT) of EXAFS spectra from biogenic uraninite and stoichiometric UO_2

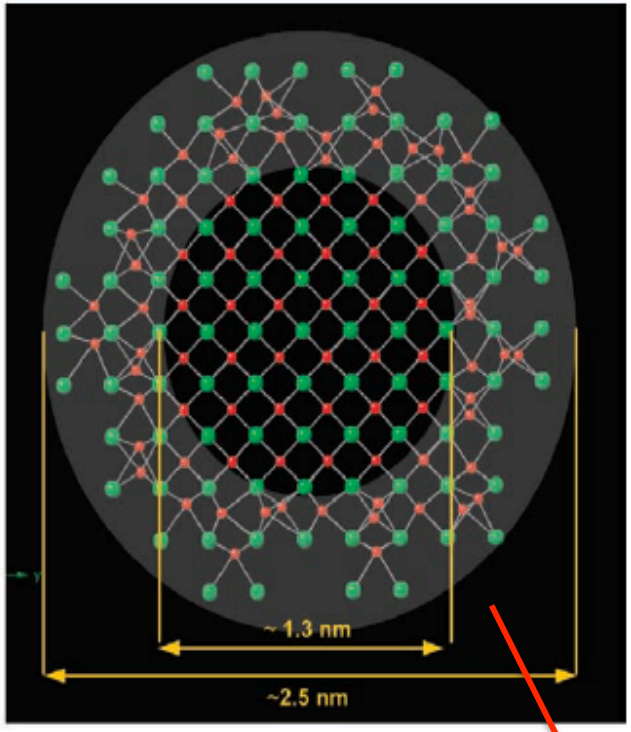

Ball-and-stick representation of the structure of biogenic uraninite nanoparticles. The shaded area emphasizes the slightly distorted outer zone of the nanoparticles.
Uranium atoms are red; oxygen atoms are green.

The lattice constant for biogenic uraninite was similar to that of bulk stoichiometric UO_2.00 (5.467 Å vs 5.468 Å), indicating that the biogenic uraninite lattice was largely unstrained. The mean particle size for the biogenic uraninite produced in this study was 2.5 nm.

Elements (2008), **4**, 407

Formation of nanocrystalline thorium bearing coffinite ((U,Th)- $SiO_4 \cdot nH_2O$, n = 0−2), measuring 20−40 nm in size.

Characteristic Th/U ratios of 0.6 associated with amorphous phases of uranium bearing thorite ((Th,U)SiO4·nH2O), having measured Th/U ratios 10 times higher.

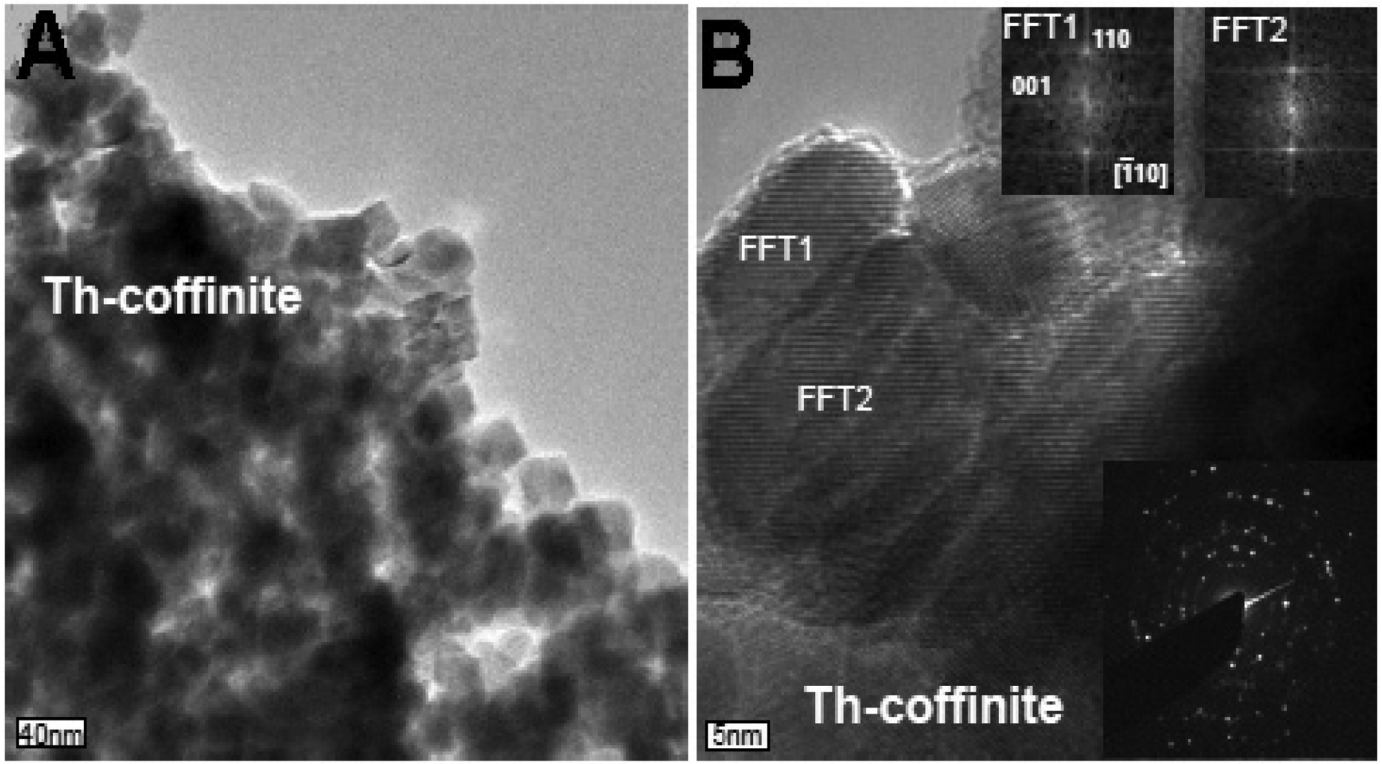

(A) HRTEM image of nanoparticles of Th-coffinite formed on U bearing thorite. (B) Higher resolution image with SAED at lower right and two FFT, indicating misalignment and similar alignment of crystals, respectively.

Chem. Rev. (2013), 113, 995

Sheets of polyhedra are by far the most common structural units, and they are often linked through low-valence cations or hydrogen bonds or in some cases through anions, resulting in a framework-like structure.

Example $MAnO_2(CO_3)$ with Np, Pu and Am

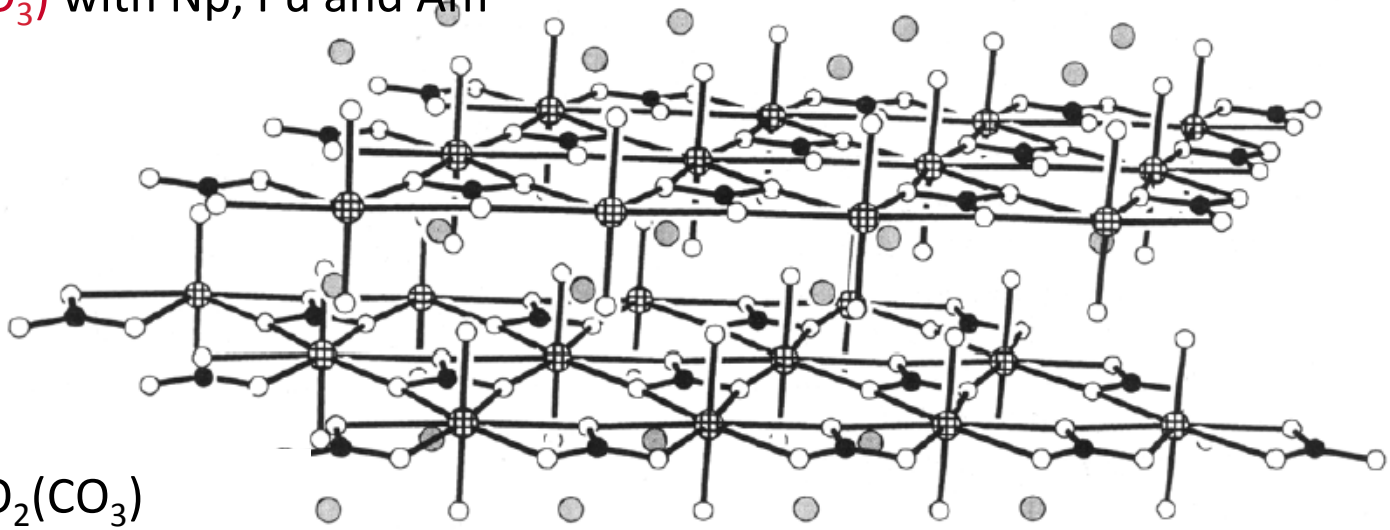

Hexagonal : $KPuO_2(CO_3)$

$M_3AnO_2(CO_3)_2$ with Np, Pu and Am and M = Na, K, Rb. Hexagonal structure

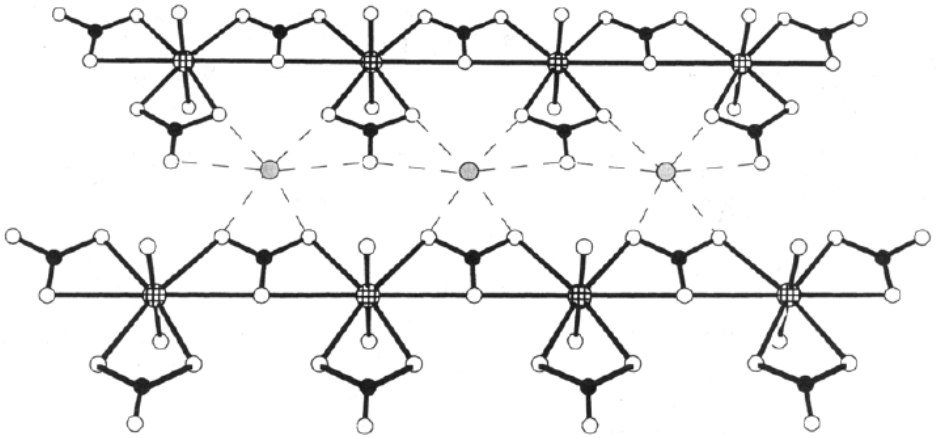

$K_3NpO_2(CO_3)_2$

D. L. Clarck et al. Chem. Rev. (1995), 95, 25

3. Speciation and specialtion tools in natural environment

Possible speciation and analytical tools

Mass spectrometry (various resolutions and configurations)
LIBS (Laser Induced Breakdown Spectroscopy)
Micro-XRD
XAS
Electron Microscopy
AFM
Radiometry

3.1 X-ray Asorption Spectroscopy

X-ray Absorption Spectroscopy is a direct speciation technique independent of the physical state of the sample and element dependent.

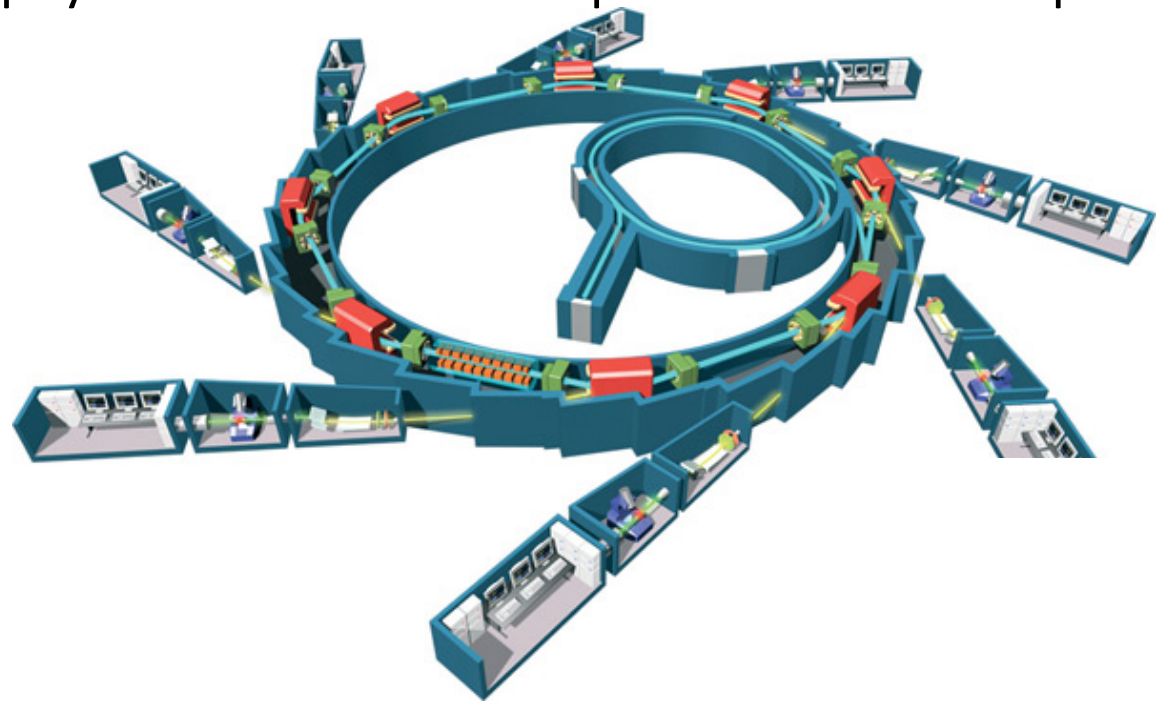

Synchrotron ring (SOLEIL, ESRF)

Beam line

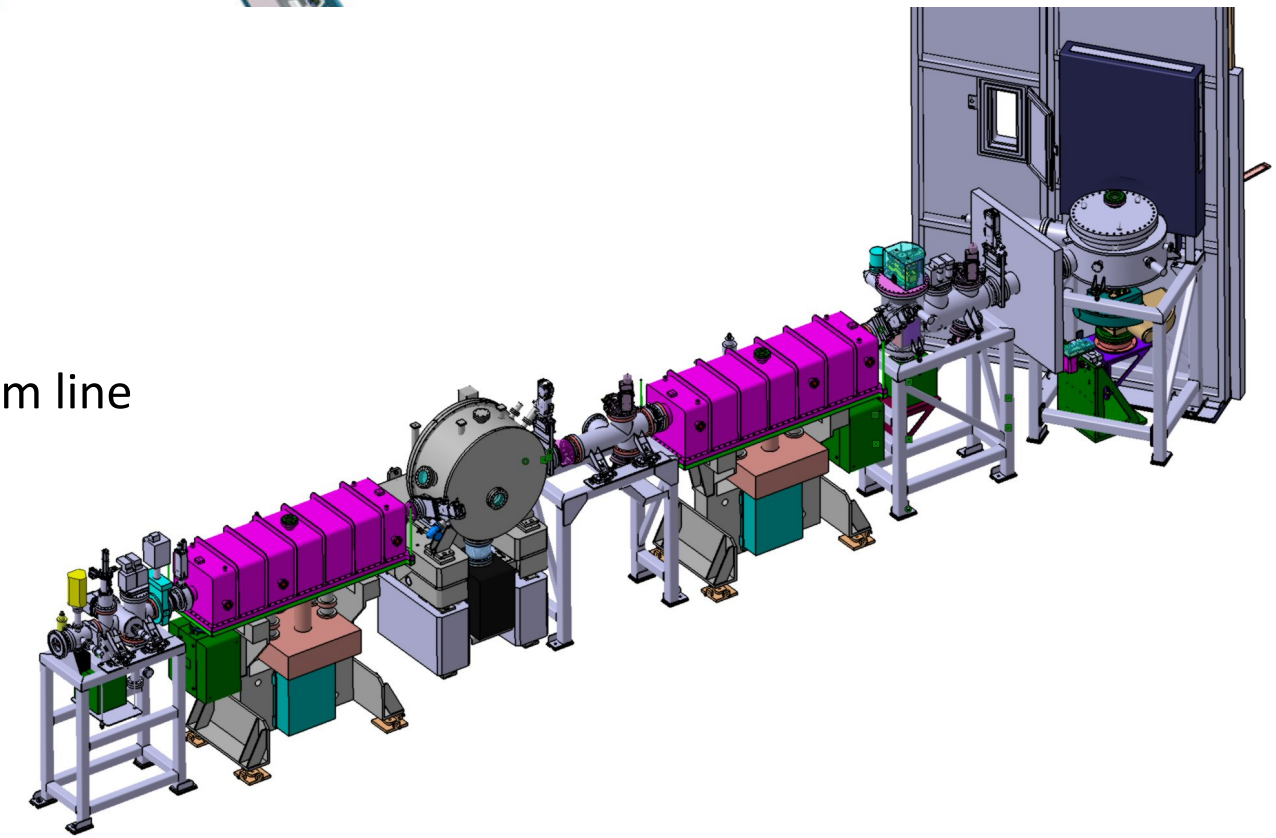

Bohr model (1913)

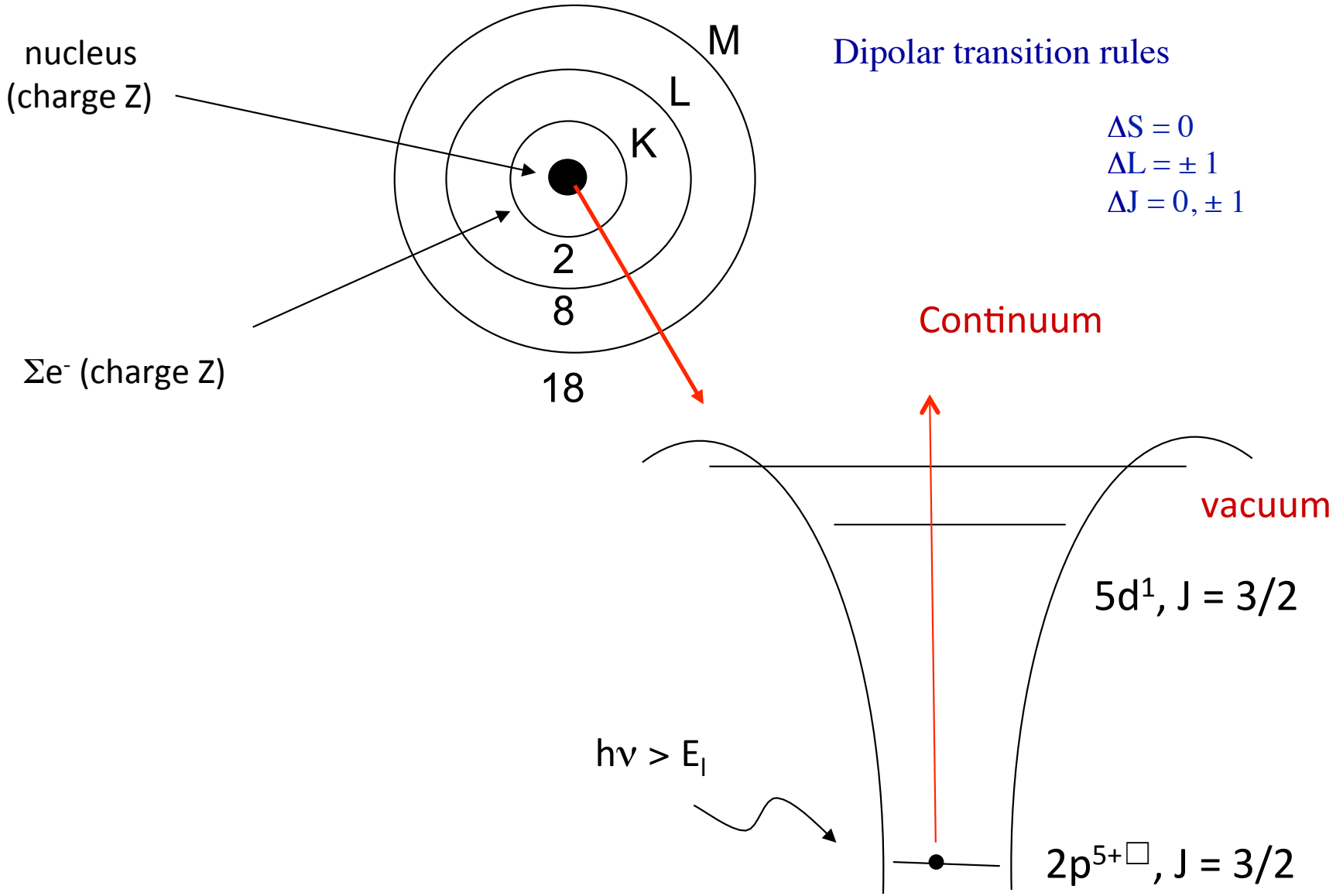

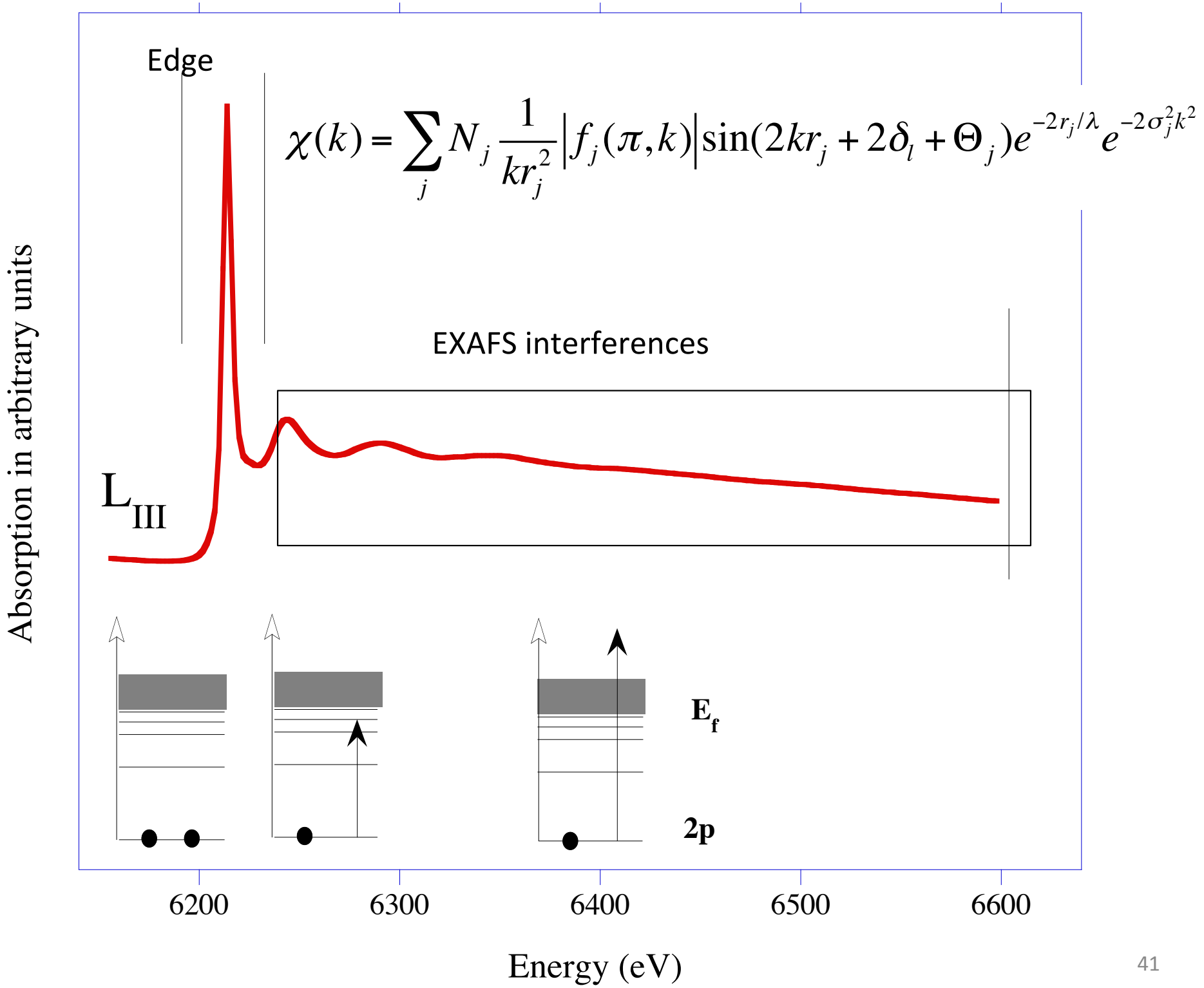
Edge
$\chi(k) = \sum_j N_j \frac{1}{kr_j^2} |f_j(\pi,k)| \sin(2kr_j + 2\delta_l + \Theta_j) e^{-2r_j/\lambda} e^{-2\sigma_j^2 k^2}$
EXAFS interferences
L_{III}
E_f
2p
Absorption in arbitrary units
6200
6300
6400
6500
6600
Energy (eV)

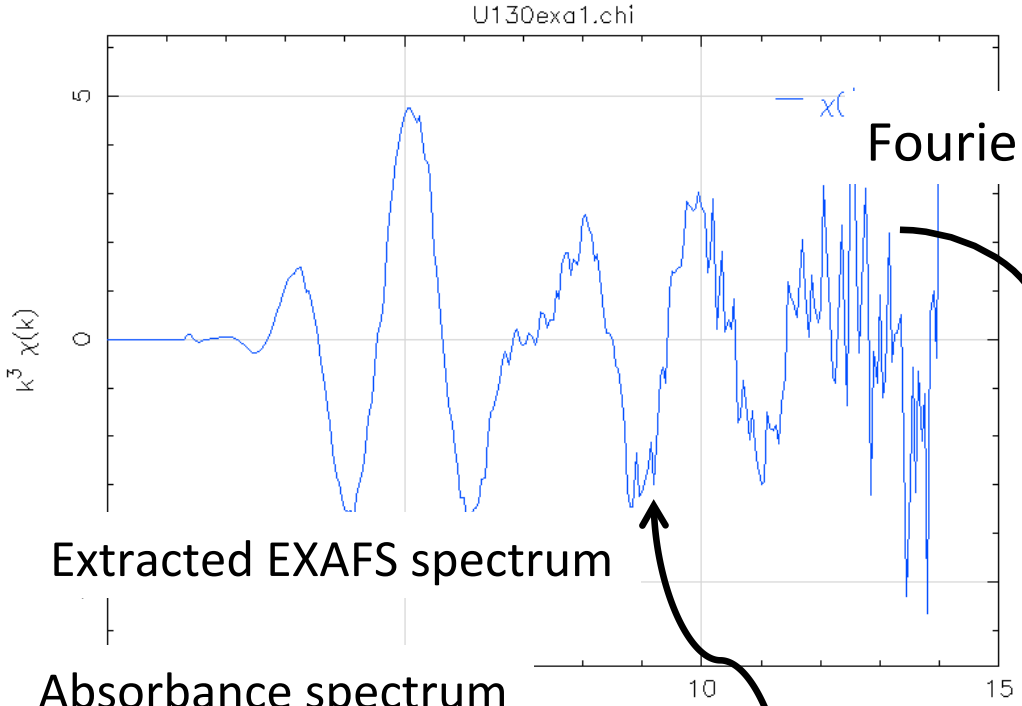

Extracted EXAFS spectrum

Fourier transform

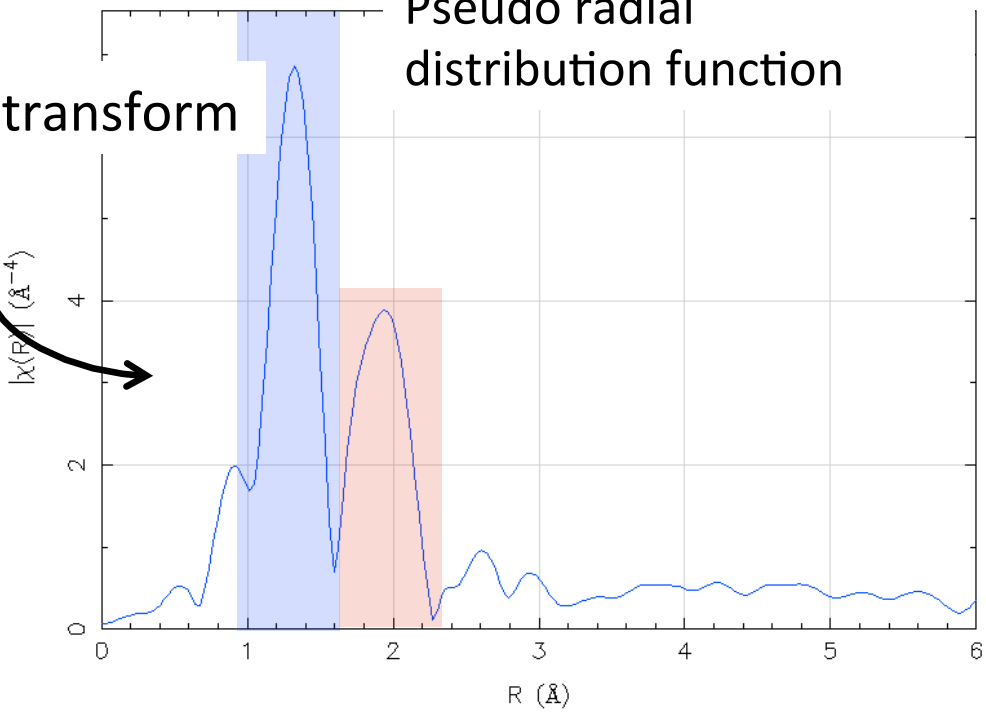

Pseudo radial distribution function

Absorbance spectrum

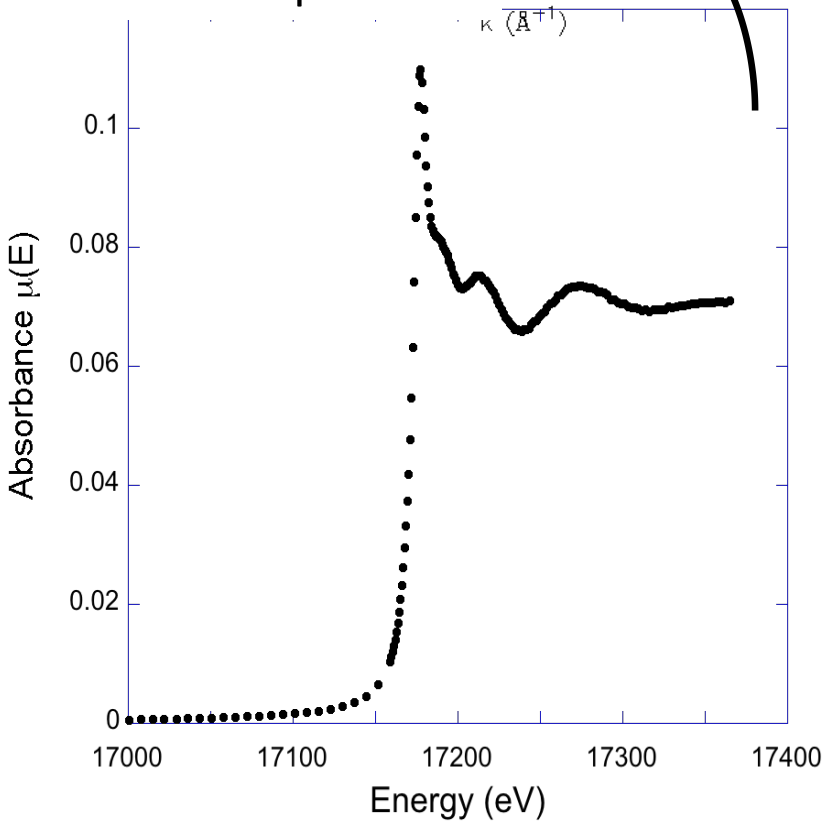

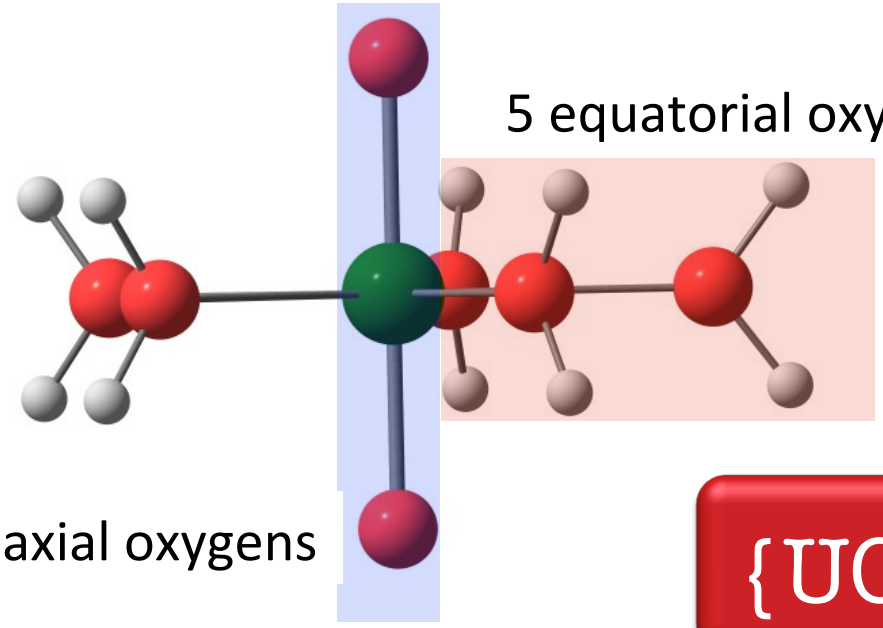

5 equatorial oxygens

2 axial oxygens

$\{UO_2^{2+}\}$

From 1952 to 1989, the Rocky Flats Plant fabricated components for the nation's nuclear weapons arsenal using various radioactive and hazardous materials.

Colorado, USA

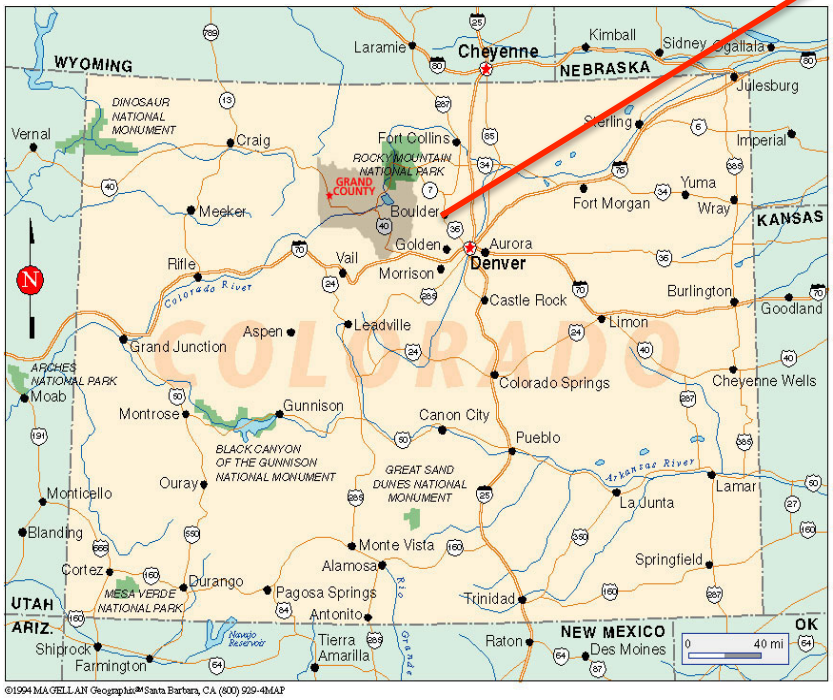

1969, aerial view of 700 area buildings (home of Pu operations). A fire in 1969 heavily damaged the interior of buildinsg 776 and 777.

« From 1958 to 1969, drums containing plutonium-contaminated lathe coolant were stored on the Pad, located on the southeastern part of the Industrial Area. These drums leaked, and wind and water erosion carried plutonium and americium in a well-defined pattern to the east and southeast, past the eastern Site boundary in some cases. Based upon material balance around the drums, it was estimated that a total of 5,000 gallons containing approximately 86 g (5.3 Ci) of plutonium were released into soils »

"hot spot" of 239/240Pu concentrations in excess of 1,000 pCi/g at the 903 Pad

A clear plume of 239/240Pu contamination that tracks roughly with the prevailing winds from NW to SE is evident from the data.

This figure represents conditions at Rocky Flats prior to soil remediation actions

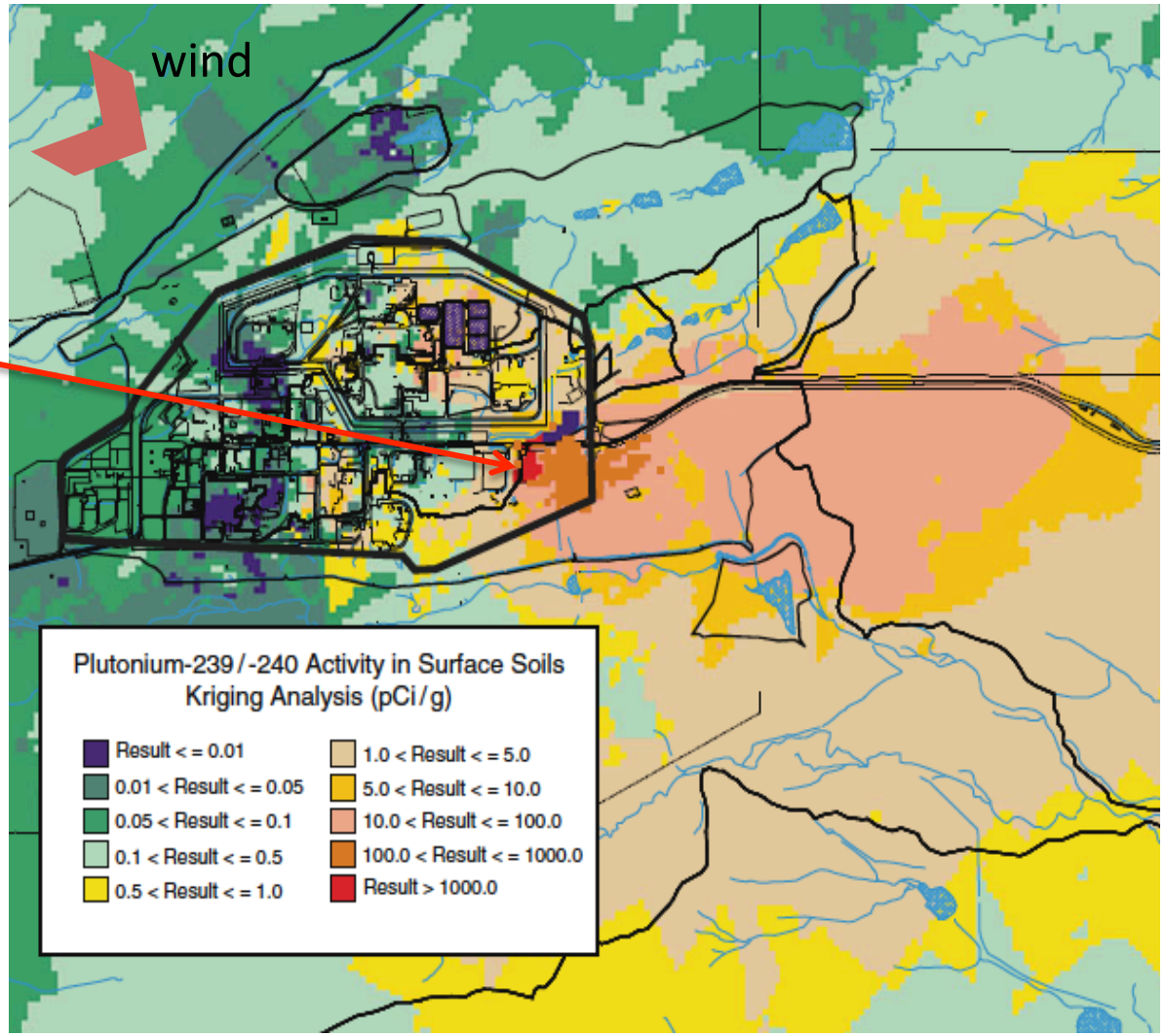

S. D. Conradson et al. , p377-398, in Actinide Nanoparticle Research, Ed. Stepan N. Kalmykov, Melissa A. Denecke, Springer (2011).

Samples from the vicinity of 903 pad

Pu is predominantly, if not entirely, Pu(IV) and exhibits the XANES signatures consistent with PuO_2 .

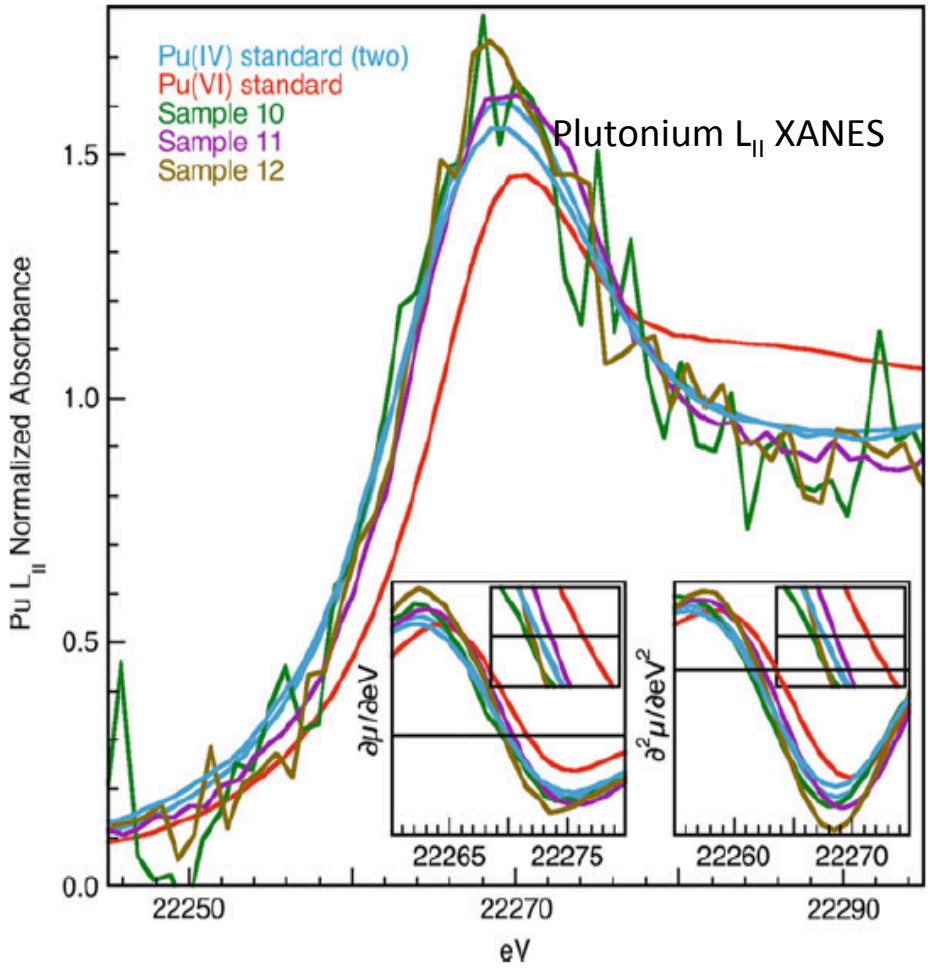

Plutonium LII XANES of Pad 903 soil samples 10, 11, and 12; insets show first (zeros 1⁄4 peak energies), left, and second (zeros 1⁄4 inflection point energies), lower right, derivatives. The boxes at extreme top-right of the insets show a higher magnification of the first derivatives' crossing of the zero line, and the second derivative at the zero line, illustrating the close coincidence of peak positions and inflection points of all spectra with that of the Pu(IV) standard

=> Particle transport mechanisms rather than aqueous sorption–desorption processes

S. D. Conradson et al. , p377-398, in Actinide Nanoparticle Research, Ed. Stepan N. Kalmykov, Melissa A. Denecke, Springer (2011).

Samples showing Pu-containing particles from the Hanford Z-9 crib

Preponderance of Pu occurs in µm-scale particles that were most likely not its original form. It suggests that Pu was mobilized and subsequently reacted, nucleating on the crystal surfaces as a surface complex.

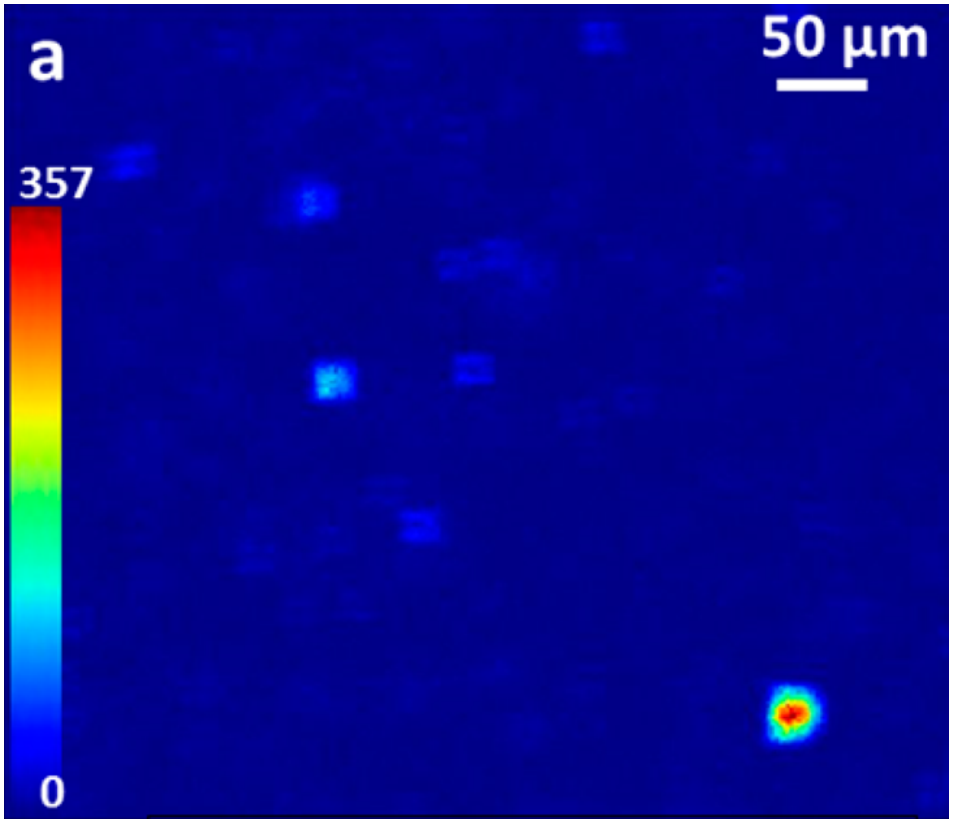

Pu map of a Hanford Z-9 crib sample (sensitivity to only Pu results from subtracting the counts measured at 18000 eV that is below the Pu L3 absorption edge from those at 18100 eV that is above it).

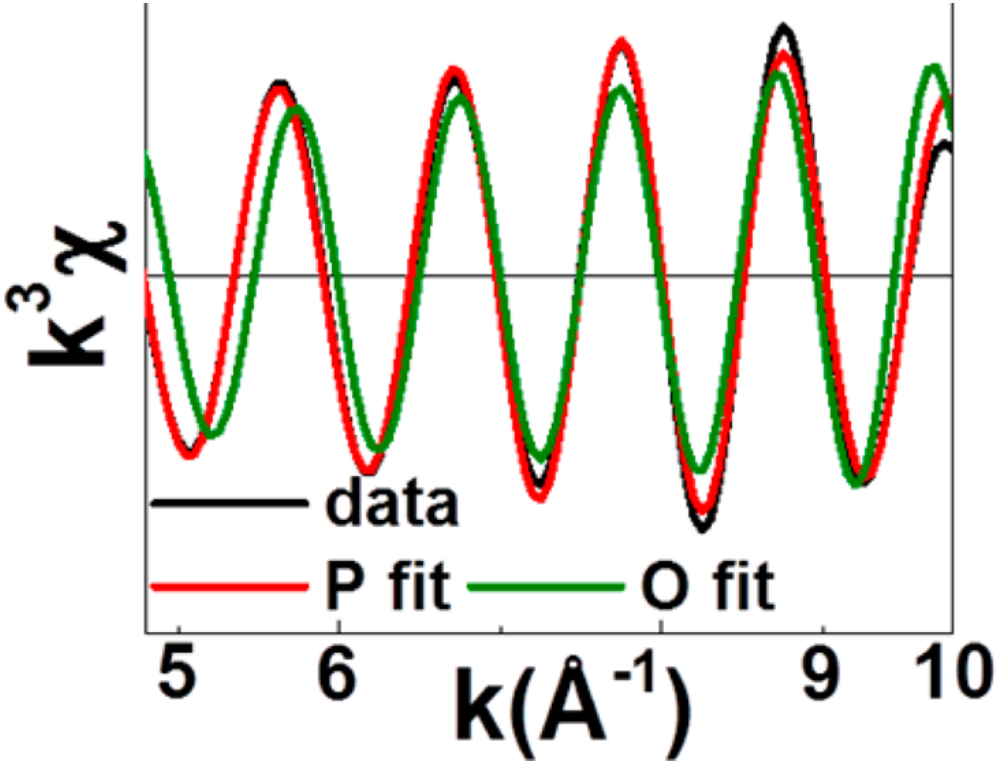

The Pu–P and Pu–O curve-fits to the Fourier filtered, non-PuO2 wave in the data, from which the much higher quality of the Pu–P fit–it is under the red line of the Pu–P fit at lower k–can be discerned.

ES&T (2015), 49, 6474

Few grams collected from one hot spot at the Los Alamos TA-21 site that most likely originated as R&D waste

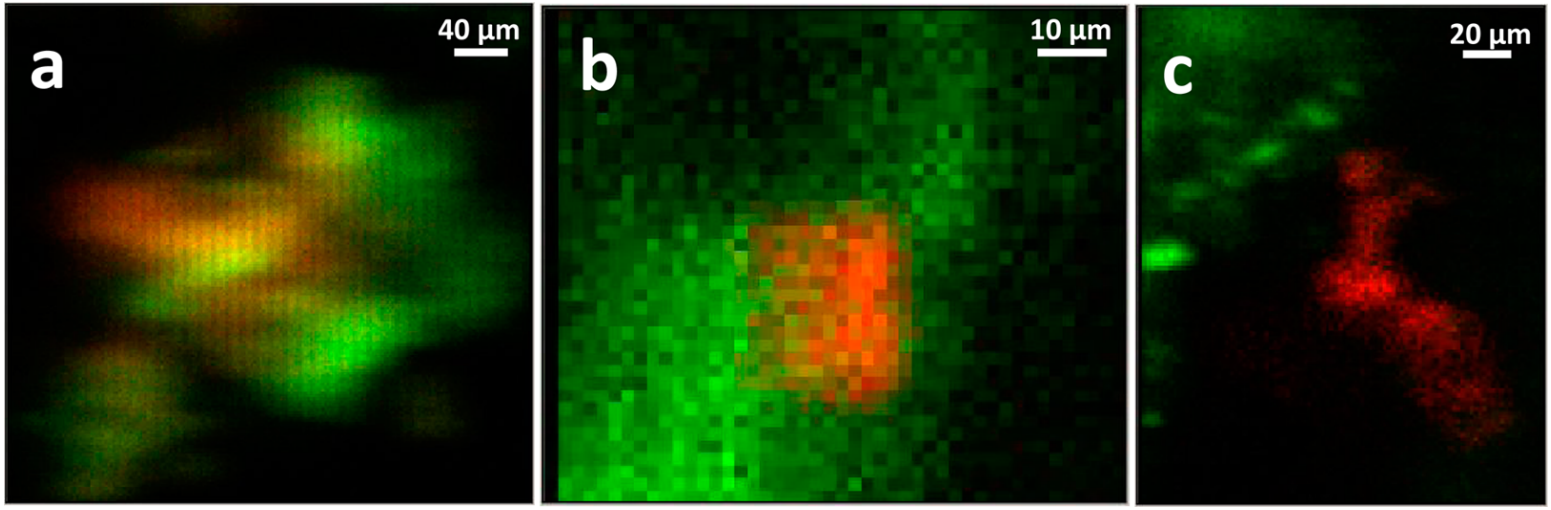

Two-color µ-XRF maps (Pu = red, Fe = green) of Los Alamos TA-21 Pu particles. (a), a mixed Pu–Fe particle, one of two found in the measured samples. (b) Pu particle on an Fe-based mineral grain, one of six similar particles. (c) separated, noncorrelated Pu and Fe particles, one of three similar particles.

=> Variation in particle composition is due to Pu deposition onto the chemically diverse soil materials when the putatively acidic solution was neutralized by reacting with the soil components

3.2 Accelerated Mass Spectroscopy

Accelerator mass spectrometry (AMS) is presently one of the most sensitive analytical techniques for the determination of heavy radionuclides

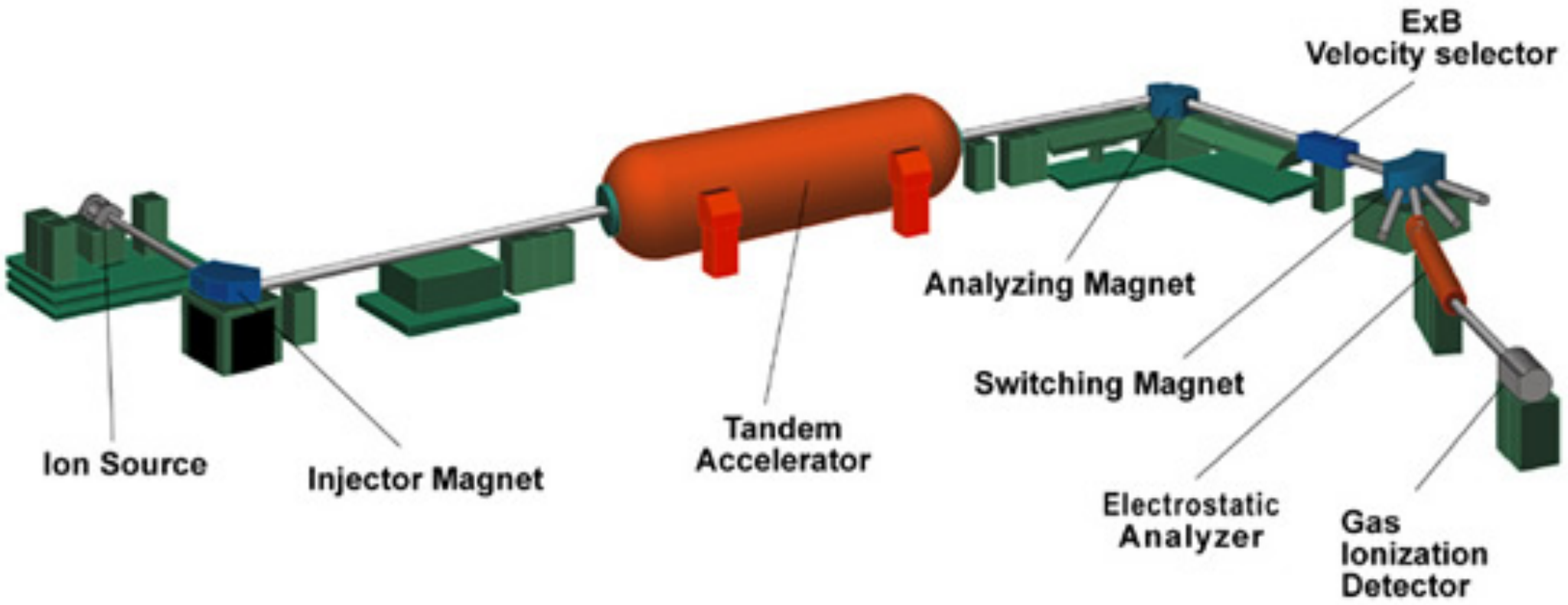

The **ion source** produces a beam of ions. from a few milligrams of solid material. Atoms are sputtered from the sample by cesium ions which are produced on a hot spherical ionizer and focused to a small spot on the sample.
Negative ions produced

The **injector magnet** bends the negative ion beam by 90° to select the mass of interest, a radioisotope of the element inserted in the sample holder, and reject the much-more-intense neighboring stable isotopes.

The **tandem accelerator** consists of two accelerating gaps with a large positive voltage in the middle. The center of the accelerator is charged to a voltage of up to 10 million volts.
The negative ions traveling down the beam tube are accelerated towards the positive terminal. At the terminal they pass through an electron stripper, either a gas or a very thin carbon foil, and emerge as positive ions.

The analyzing and switching magnets eliminate molecules completely by selecting only the highly charged ions that are produced in the terminal stripper.

The **gas ionization detector** counts ions one at a time as they come down the beamline. The ions are slowed down and come to rest in propane gas. As they stop, electrons are knocked off the gas atoms. These electrons are collected on metal plates, amplified, and read into the computer.

Determination of 236-U, 237-Np, 239-Pu and, where detectable, 240-Pu in various natural water samples by using 233-U as Chemichal Ionization Yield tracer

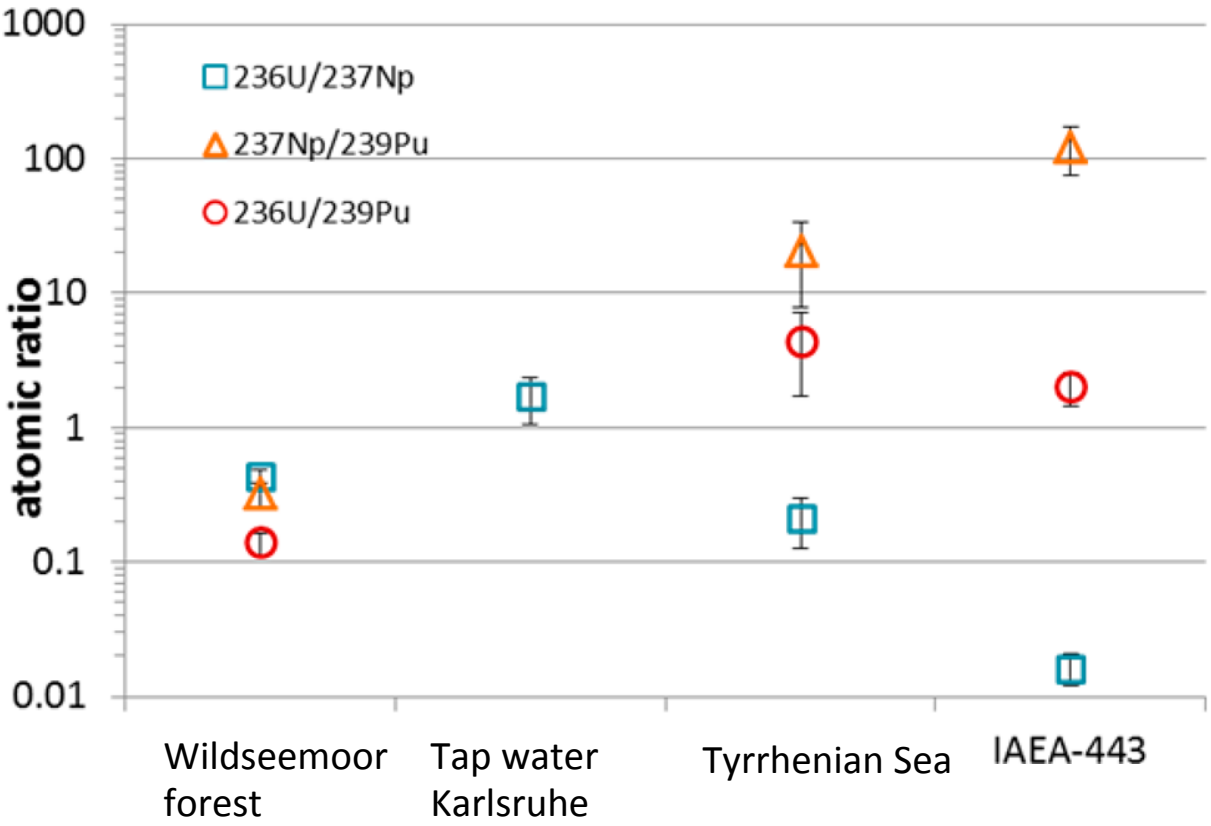

Sample mass = 100 – 250 g

236U/237Np, 237Np/239Pu, and 236U/239Pu atomic ratios measured in four different natural water samples of mass between 100 and 250 g. This figure shows how the observed atomic ratios reflect both the contamination source and the different behavior of U, Np, and Pu in the investigated environmental system.

Anal. Chem. (2015), 87, 5766

IAEA - 443 } Seallafiled Reprocessing plant

Karlsruhe tap water
Wildseemoor Forest
Tyrrhenian Sea
} Global fallout

=> reflect the different behavior of the investigated actinides in three environmental systems.

✔ Highest ratio of Np/Pu Δ and U/Pu **O** in Tyrrhenian Sea compared to Wildseemoor Forest
reflects the higher mobility of U and Np compared to Pu.

✔ In surface water rich in high dossilved organic carbon (Wildseemoor sample), the atomic ratios of the three nuclides are comparable.

✔ In the tap water Karlsruhe sample, a higher mobility of U □ with respect to Np is observed compared to the organic-rich surface water Wildseemoor sample.

✔ The isotopic ratio 240-Pu/239-Pu = 0.17 ± 0.04 could also be determined. This value is consistent with the global fallout origin of the Pu contamination.

3.3 The specific case of seawater

Ionic strength in seawater stands at about 0.60 mol L1 (35 g/L NaCl), average pH of around 8.2.
E_h between 0.2 and 0.3 mV

✔ For Pu, various reports -> "the predominance of Pu(V) *should* truly be observed in seawater"

Predictive calculations :

PuO_2^+ (69.9%), PuO_2Cl (18.3%), $PuO_2SO_4^{2-}$ (6.0%), $PuO_2CO_3^{2-}$ (5.3%).

But no experimental evidence for now

✔ For U, the "dominant aqueous uranium(VI) species under seawater conditions is the neutral $[Ca_2UO_2(CO_3)_3](aq)$".

✔ For Np, should be similar to Pu but no real data

✔ For Am, should be similar to the lanthanides

Journal of Radioanalytical and Nuclear Chemistry, Vol. 251, No. 2 (2002) 213
Journal of Environmental Radioactivity 153 (2016) 237
Chem. Eur. J. 2014, 20, 14499

Uranium, EXAFS, L_{III} edge

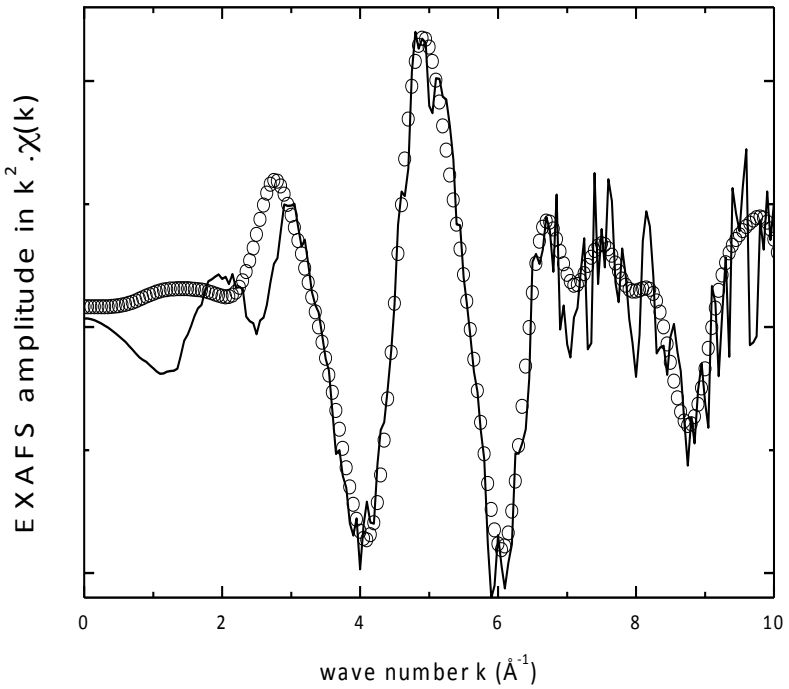

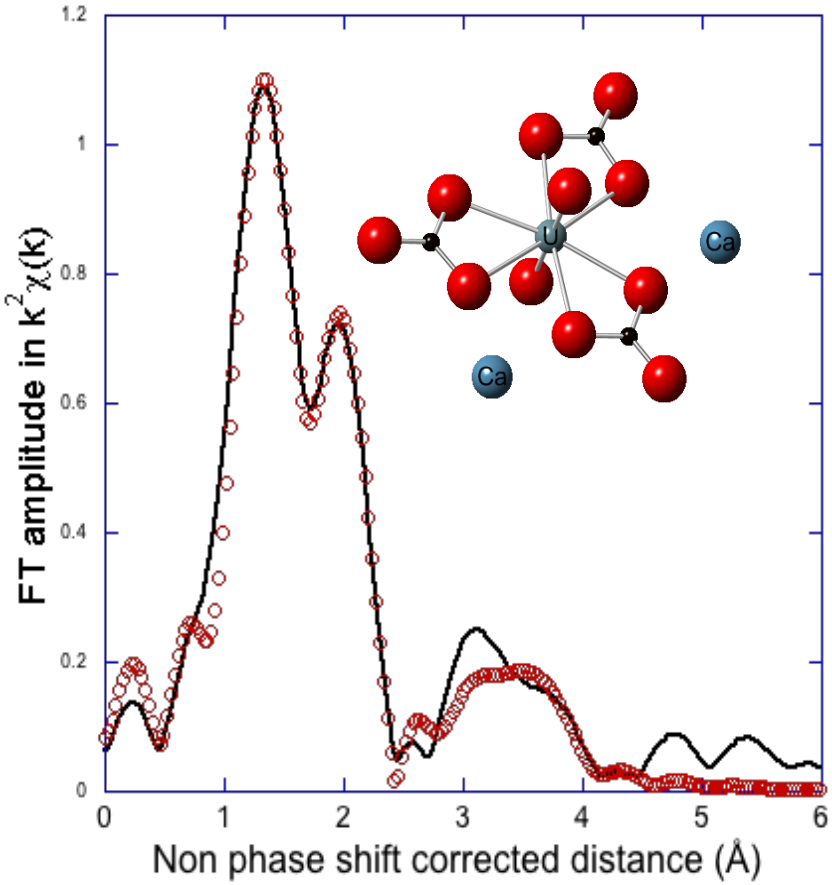

$Ca_2UO_2(CO_3)_3.nH_2O$

2 U - O_{ax} at **1.80**(1) Å, σ^2=0.0013 Å²
5.8(5) U - O_{eq} at **2.43** (1) Å, σ^2=0.095 Å²
2.9(3) U-C at **2.90**(1) Å, σ^2=0.0060 Å²

S_0^2 = 1.0, e_0 = -1.70 eV, R-factor = 1.5%

Model : Liebigite $Ca_2UO_2(CO_3)_3.11H_2O$

Bernhard et al. Radiochimica Acta 74, 87 (2001)
Dalton Trans. (2015), 44, 5417

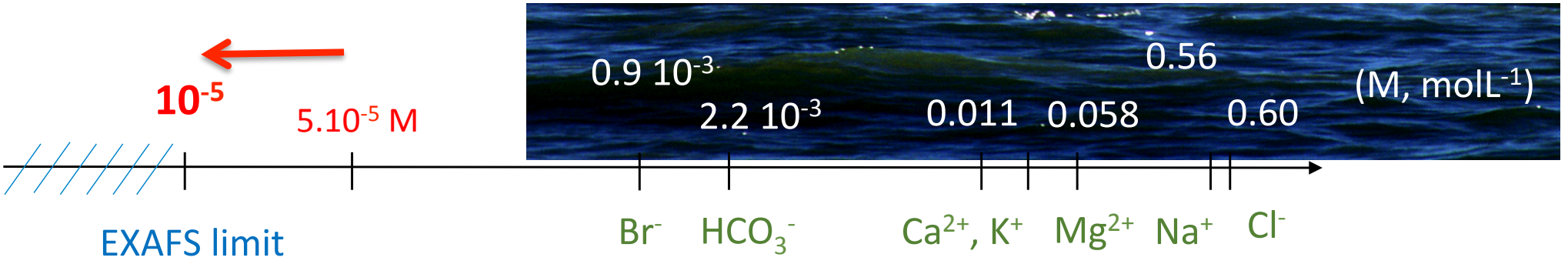

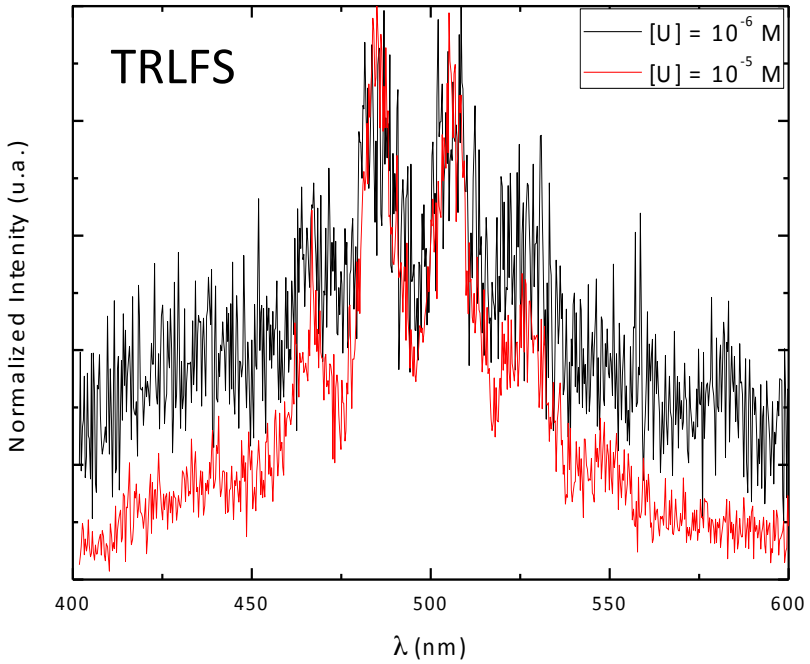

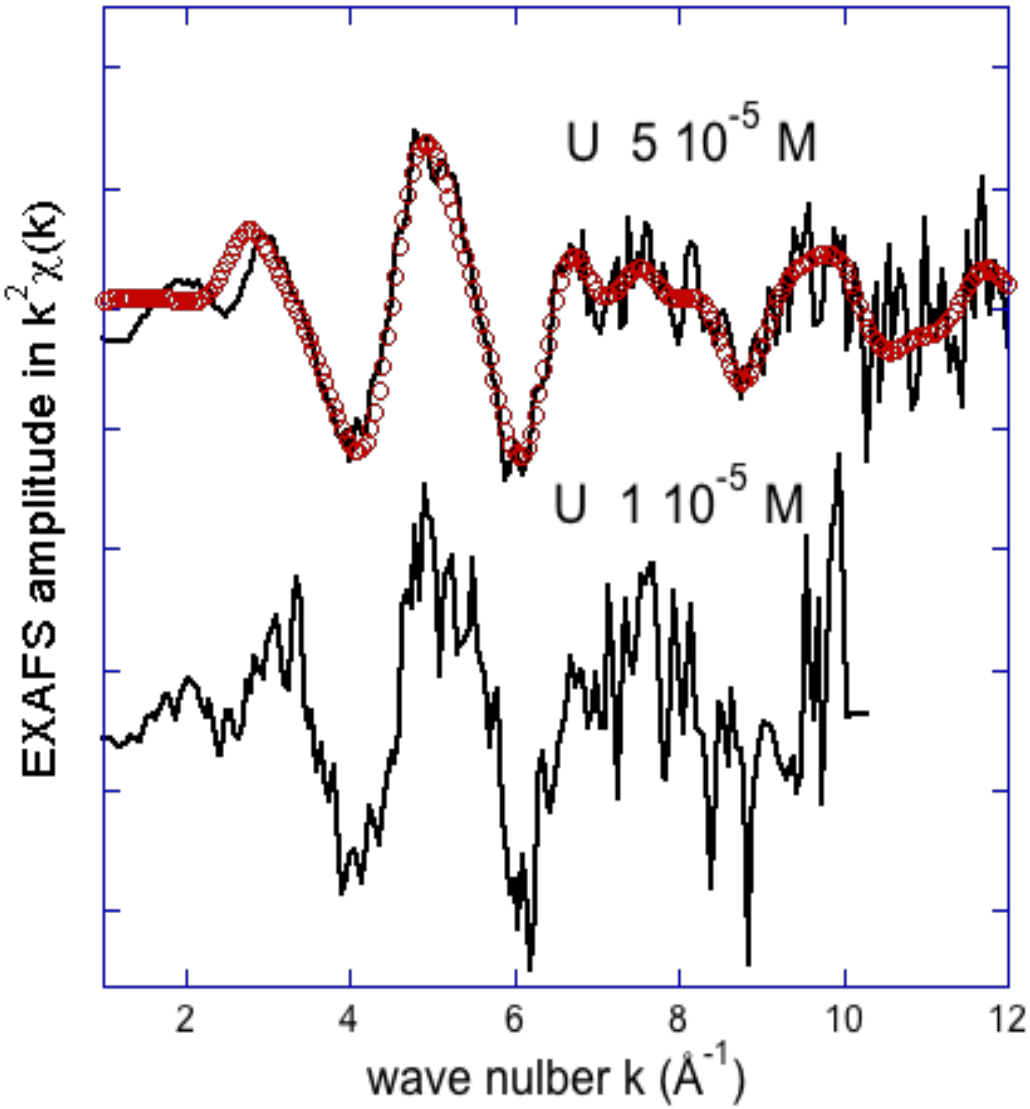

No difference in speciation

Confirms simulation data

Dalton Trans. (2015), 44, 5417

Américium

Speciation modeling

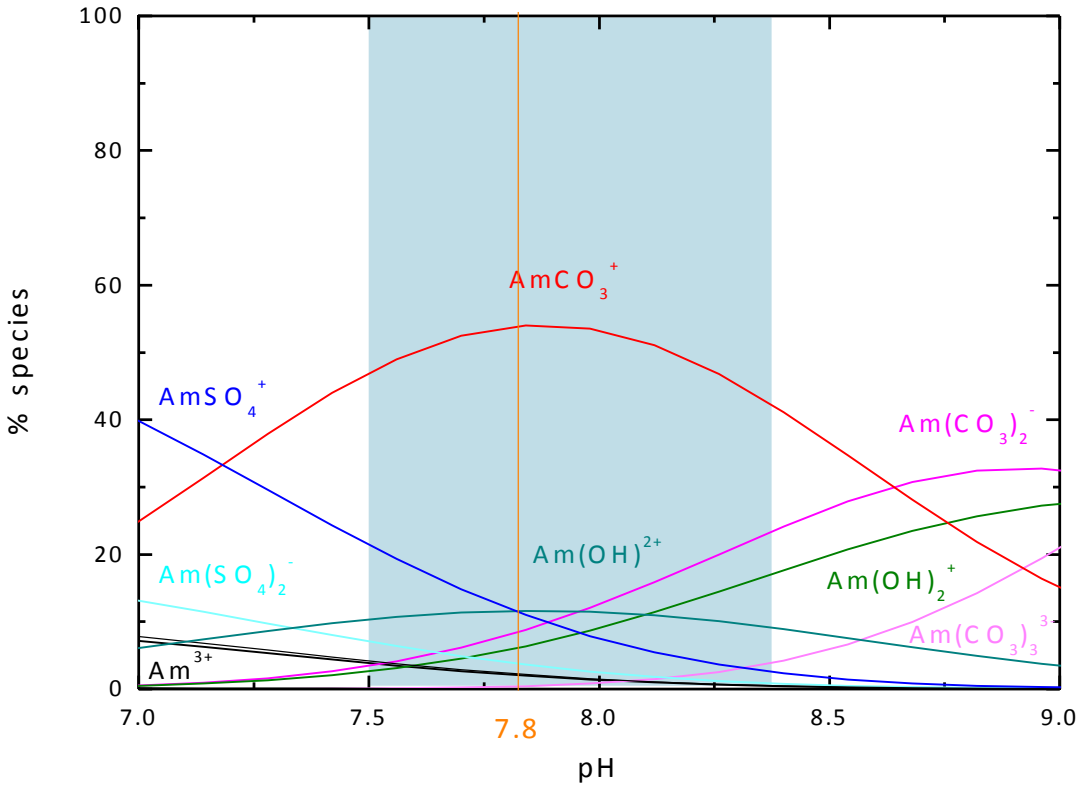

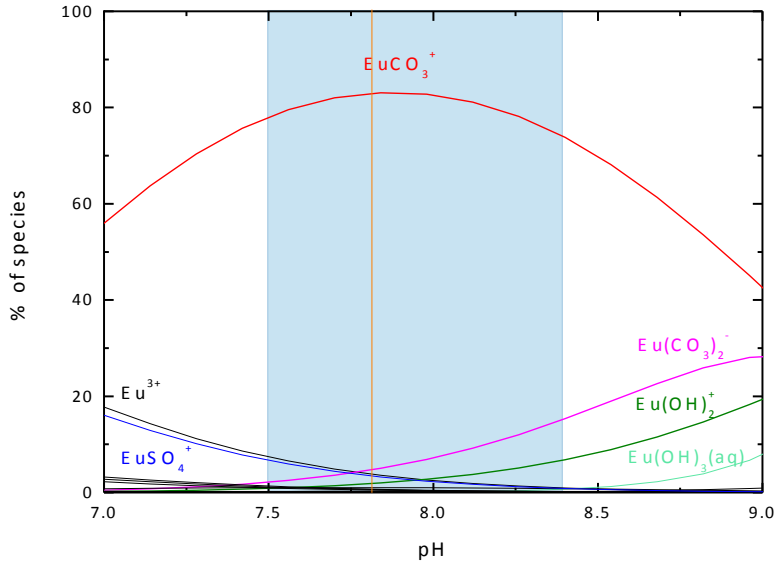

Prediction speciation diagrams of americium at 5x10^{-5} M (a) and europium at 5x10^{-5} M (b) in seawater (JCHESS®)

Am, Eu, EXAFS, L_{III} edge

$NaAm(CO_3)_{mon\ 2}.nH_2O$

$NaEu(CO_3)_{bid2}.nH_2O$

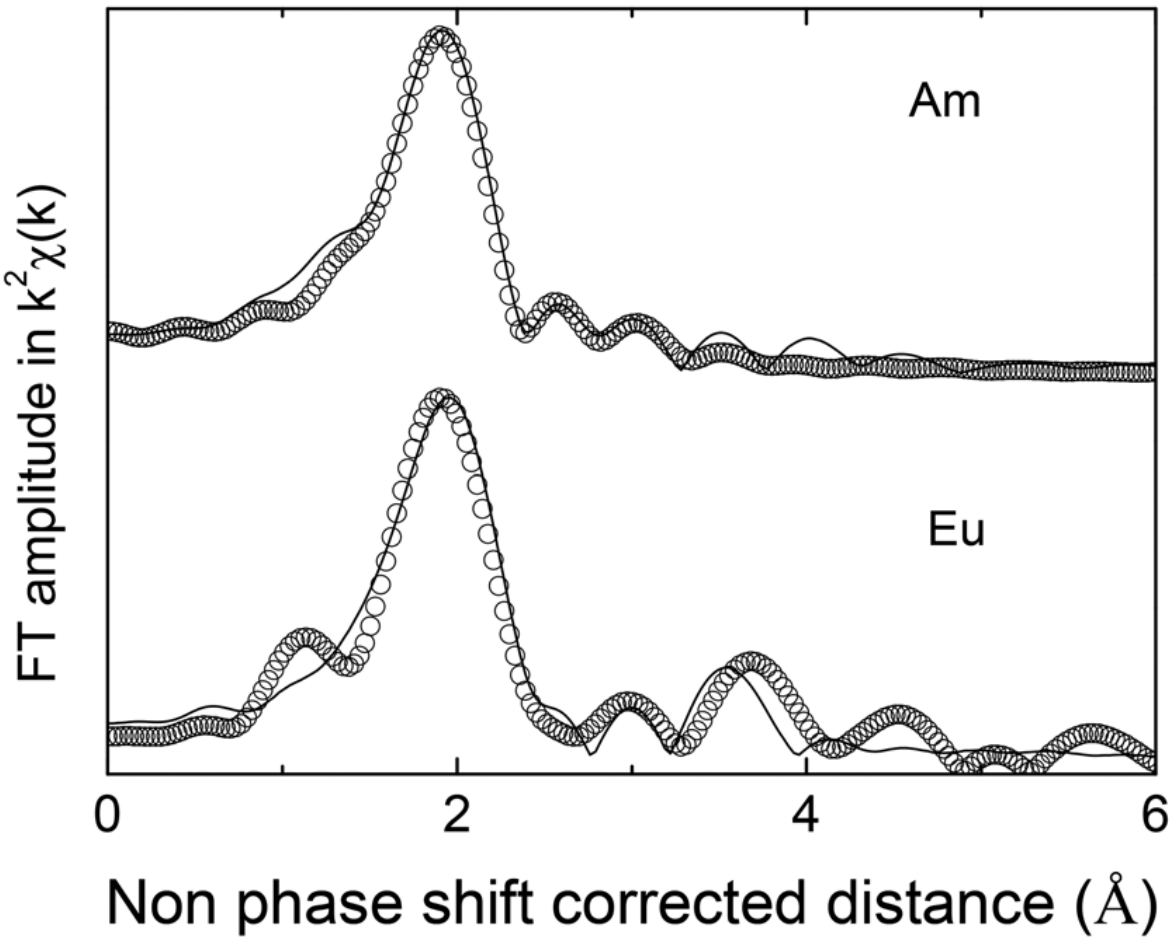

Corresponding Fourier transform of the EXAFS spectrum of the doped seawater solution at 5 × 10−5 M. Experimental spectra in black lines, adjustment in dots.

9 $O_{(carb+wat)}$ at **2.48**(1) Å, σ^2 = 0.0094 Å²
1 Na at **3.71**(9) Å, σ^2 = 0.0066 Å²
2 C_{carb} at **3.73**(3) Å, σ^2 = 0.0049 Å²

S_0^2 = 1.1, e_0 = -5.83 eV, R-factor = 1.2 %

Dalton Trans., 2015, 44, 20584